Mechanistic Studies of the Dehydrocoupling and Dehydropolymerization of Amine−Boranes Using a [Rh(Xantphos)]+ Catalyst

Heather C. Johnson,[†] Erin M. Leitao,[‡] George R. Whittell,[‡] Ian Manners,*,[‡] Guy C. Lloyd-Jones,*,[§] and Andrew S. Weller*,[†]

[†]Department of Chemistry, Chemistry Research Laboratories, University of Oxford, Mansfield Road, Oxford OX1 3TA, United Kingdom

[‡]School of Chemistry, University of Bristol, Cantock's Close, Bristol BS8 1TS, United Kingdom

[§]School of Chemistry, University of Edinburgh, West Mains Road, Edinburgh EH9 3JJ, United Kingdom

Ⓢ Supporting Information

ABSTRACT: A detailed catalytic, stoichiometric, and mechanistic study on the dehydrocoupling of $H_3B\cdot NMe_2H$ and dehydropolymerization of $H_3B\cdot NMeH_2$ using the $[Rh(Xantphos)]^+$ fragment is reported. At 0.2 mol % catalyst loadings, dehydrocoupling produces dimeric $[H_2B-NMe_2]_2$ and poly(methylaminoborane) ($M_n = 22\,700$ g mol^{-1}, PDI = 2.1), respectively. The stoichiometric and catalytic kinetic data obtained suggest that similar mechanisms operate for both substrates, in which a key feature is an induction period that generates the active catalyst, proposed to be a Rh−amido−borane, that reversibly binds additional amine−borane so that saturation kinetics (Michaelis−Menten type steady-state approximation) operate during catalysis. B−N bond formation (with $H_3B\cdot NMeH_2$) or elimination of amino−borane (with $H_3B\cdot NMe_2H$) follows, in which N−H activation is proposed to be turnover limiting (KIE = 2.1 ± 0.2), with suggested mechanisms that only differ in that B−N bond formation (and the resulting propagation of a polymer chain) is favored for $H_3B\cdot NMeH_2$ but not $H_3B\cdot NMe_2H$. Importantly, for the dehydropolymerization of $H_3B\cdot NMeH_2$, polymer formation follows a chain growth process from the metal (relatively high degrees of polymerization at low conversions, increased catalyst loadings lead to lower-molecular-weight polymer), which is not living, and control of polymer molecular weight can be also achieved by using H_2 ($M_n = 2\,800$ g mol^{-1}, PDI = 1.8) or THF solvent ($M_n = 52\,200$ g mol^{-1}, PDI = 1.4). Hydrogen is suggested to act as a chain transfer agent in a similar way to the polymerization of ethene, leading to low-molecular-weight polymer, while THF acts to attenuate chain transfer and accordingly longer polymer chains are formed. In situ studies on the likely active species present data that support a Rh−amido−borane intermediate as the active catalyst. An alternative Rh(III) hydrido−boryl complex, which has been independently synthesized and structurally characterized, is discounted as an intermediate by kinetic studies. A mechanism for dehydropolymerization is suggested in which the putative amido−borane species dehydrogenates an additional $H_3B\cdot NMeH_2$ to form the "real monomer" amino−borane $H_2B=NMeH$ that undergoes insertion into the Rh−amido bond to propagate the growing polymer chain from the metal. Such a process is directly analogous to the chain growth mechanism for single-site olefin polymerization.
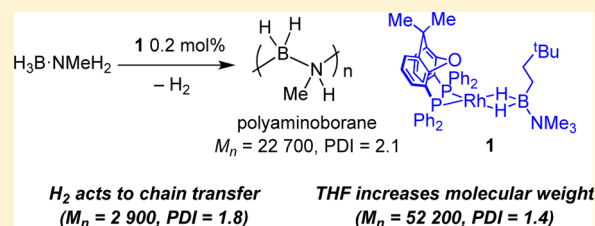
1. INTRODUCTION

Catalytic routes for the formation of main-group/main-group bonds are important for the targeted construction of new molecules and materials. However, enabling catalytic methodologies for such bond-forming events lag behind those developed for the construction of C−C and C−X bonds.[1] The development of reliable, robust, and controllable processes is thus an important challenge.[2−5] Catalytic dehydropolymerization[6] of amine−boranes to give polyaminoboranes presents one such opportunity, as this produces new BN polymeric materials that are isoelectronic with technologically pervasive polyolefins. Such new materials have potential applications as high-performance polymers and as precursors to BN-based ceramics and single-layer hexagonal BN thin films (white

graphene).[7] Although ill-defined branched, oligomeric materials that have been termed "polyaminoborane" have historically been prepared by noncatalytic methods,[8−11] it is only recently that high-molecular-weight, essentially linear polyaminoboranes have been produced by catalytic methods from amine−boranes such as $H_3B\cdot NH_3$ and $H_3B\cdot NMeH_2$ (Scheme 1), initially using Brookhart's catalyst $Ir(^tBuPOCOP^tBu)H_2$ [$^tBuPOCOP^tBu = \kappa^3\text{-}_{PCP}\text{-}1,3\text{-}(OP^tBu_2)_2C_6H_3$].[12]

In 2006, Goldberg, Heinekey, and co-workers demonstrated that $H_3B\cdot NH_3$ could be dehydrooligomerized using this Ir catalyst to afford an insoluble material tentatively reported as

Scheme 1. Dehydropolymerization of Amine−Boranes Using the Ir(^{t}BuPOCOP^{t}Bu)H$_2$ Catalyst
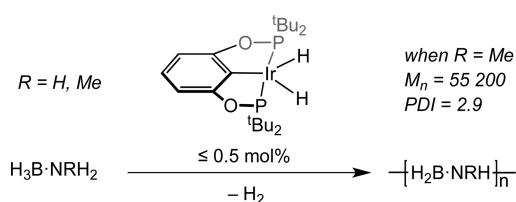
$[H_2BNH_2]_5$[13,14] but later assigned as linear polyaminoborane $[H_2BNH_2]_n$ (n = ca. 20) on the basis of solid-state ^{11}B NMR spectroscopy by Manners and co-workers.[15] In 2008, the former group[16] also described that the dehydrooligomerization of H$_3$B·NMeH$_2$ at low relative concentrations of amine−borane, or mixtures of the latter with H$_3$B·NH$_3$, gave low-molecular-weight but soluble oligomers (M_n less than ca. 2500 g mol^{-1}). Independently, in 2008, Manners and co-workers[17] reported the production of high-molecular-weight $[H_2BNMeH]_n$ (M_n = 55 200 g mol^{-1}, PDI = 2.9) and related materials at low catalyst loadings (0.3 mol %) using both high and low concentrations of substrates.[15,17] More recently, photoactivated catalysts based upon $[CpFe(CO)_2]_2$ have been reported to dehydropolymerize H$_3$B·NMeH$_2$ to $[H_2BNMeH]_n$ (M_n = 64 500 g mol^{-1}, PDI = 1.83),[18] as have Mn(η^5-C$_5$H$_5$)(CO)$_3$, Cr(η^6-C$_6$H$_6$)(CO)$_3$, and Cr(CO)$_6$ for the cases of H$_3$B·NRH$_2$ (R = Me or Et) under similar conditions.[19,20] Catalysts based upon $[Rh(Ph_2P(CH_2)_4PPh_2)]^+$ also show good activities (0.2 mol %) in producing high-molecular-weight poly(methylaminoborane), $[H_2BNMeH]_n$, from H$_3$B·NMeH$_2$ (M_n = 144 000 g mol^{-1}, PDI = 1.25).[21] Fe(PhNCH$_2$CH$_2$NPh)-(Cy$_2$PCH$_2$CH$_2$PCy$_2$)[22] and complexes based upon "bifunctional" Ru(PNP)(H)(PMe$_3$) [PNP = HN(CH$_2$CH$_2$P^{i}Pr$_2$)$_2$][23] also catalyze polyaminoborane formation, the latter at very low (less than 0.1 mol %) loadings. Ionic liquids have also been shown to support the formation of polyaminoboranes from H$_3$B·NH$_3$ when used in conjunction with metal-based catalysts.[24] It is also noteworthy that anionic oligomerization approaches to both linear and branched short-chain amino-boranes have recently been described.[25,26]

Mechanistic studies focusing on the dehydropolymerization of H$_3$B·NMeH$_2$ or H$_3$B·NH$_3$ substrates are few in number. Nevertheless, important observations and overarching rationales have been suggested from these studies. This relative dearth can be compared to studies with H$_3$B·NMe$_2$H, which are considerably more numerous, and often demonstrate subtle differences in likely mechanistic pathways depending on identity of the metal−ligand fragment.[2,18,27−33] The polymer growth kinetics (molecular weight versus conversion) using the Ir(^{t}BuPOCOP^{t}Bu)H$_2$/H$_3$B·NMeH$_2$ system suggest the operation of a modified chain-growth mechanism that involves both a slow metal-based dehydrogenation of amine−borane and faster insertion/polymerization of the resulting amino−borane.[15] By using the same system, σ-bound amine−borane intermediates for catalytic redistribution of oligomeric diborazanes have recently been proposed on the basis of kinetic modeling.[34] By using catalyst systems based upon Fe-(PhNCH$_2$CH$_2$NPh)(Cy$_2$PCH$_2$CH$_2$PCy$_2$)/H$_3$B·NH$_3$, an initiation mechanism that invokes an Fe−amido−borane has been suggested, which then undergoes dehydrogenative insertion of additional H$_3$B·NH$_3$ to form polyaminoborane.[22] For Ru-(PNP)(H)(PMe$_3$)/H$_3$B·NH$_3$, a mechanism is proposed, based upon experimental and density functional theory studies, in which amino−borane is formed in a low but steady-state concentration that undergoes catalyzed polymerization by an enchainment reaction that relies upon metal−ligand cooperatively.[23] Kinetic studies using the Ir(^{t}BuPOCOP^{t}Bu)H$_2$[16] and Ru(PNP)(H)(PMe$_3$)[23] systems demonstrate a first-order dependence on both amine−borane and catalyst concentrations, although for the latter catalyst when H$_3$B·ND$_3$ was used, there was a zero-order dependence on this substrate suggesting a change in the turnover-limiting step. A number of apparently homogeneous[35] catalyst systems show kinetic profiles that might suggest induction periods prior to rapid dehydropolymerization of H$_3$B·NH$_3$ or H$_3$B·NMe$_2$H,[14,21−23] although the underlying reasons for this have only been addressed in detail for a dehydocoupling catalyst based upon Shvo's catalyst that produces borazine rather than polyaminoborane.[36]

The role of free, transient,[38] amino−borane in dehydropolymerization, such as H$_2$B=NH$_2$ or H$_2$B=NMeH, which arises from initial dehydrogenation of amine−borane, has attracted particular attention as these (or very closely related metal-bound species) are likely boron-containing intermediates. Baker, Dixon, and co-workers have suggested that selectivity in the dehydropolymerization of H$_3$B·NH$_3$ depends on whether the intermediate amino−borane remains associated with the metal.[37] Release from the metal ultimately results in the formation of borazine by trimerization, whereas if strong coordination/rapid insertion of amino−borane into the growing polymer chain occurs, then polymerization is favored (Scheme 2). The generation of transient amino−boranes, such

Scheme 2. Suggested Pathways for Dehydropolymerization, Dehydrogenation, and Hydroboration[a]

On−Metal Dehydropolymerization

Off−Metal Dehydrocoupling

[a]Adapted from ref 37.
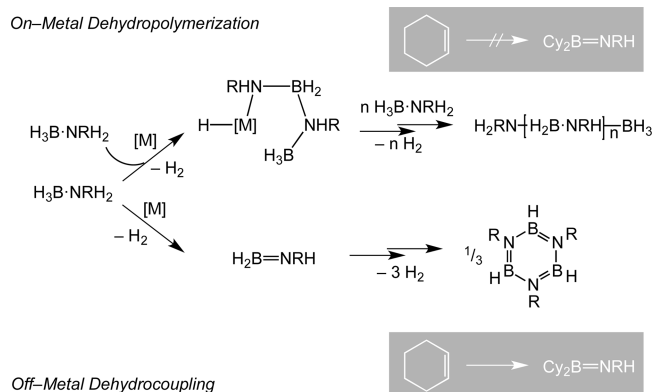
as H$_2$B=NH$_2$ or H$_2$B=NMeH, during catalysis can also be probed by addition of exogenous cyclohexene, which undergoes hydroboration to form Cy$_2$B=NHR (R = Me, H).[37] Catalyst systems in which amino−borane is suggested to not be released from the metal do not form the hydroborated product during dehydropolymerization, while for those that form borazine from trimerization of free amino−borane, or when amino−borane is produced thermally in the absence of a metal−ligand fragment,[34] the hydroborated product is observed in significant quantities. However, recent experimental and computational studies using Ir(^{t}BuPOCOP^{t}Bu)H$_2$ or Ru(PNP)(H)(PMe$_3$) suggest that, if hydroboration or borazine formation are not kinetically competitive with metal-promoted B−N coupling, then Cy$_2$B=NH$_2$ will not be observed, even if free amino−borane is formed transiently.[23,34] Adding to this complexity,

Scheme 3. Isolated Intermediates in Amine−Borane and Related Dehydrocoupling[a]
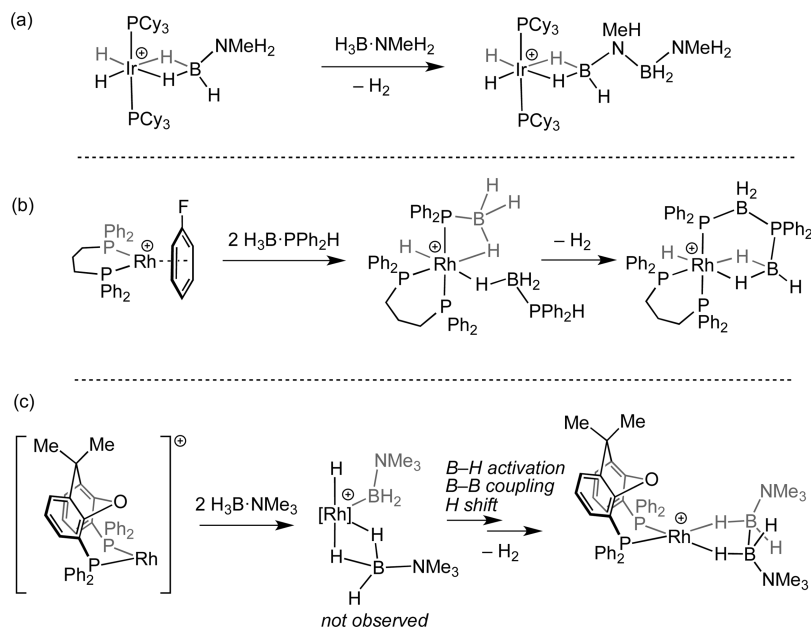
[a][BAr$^F_4$]$^-$ anions are not shown. (a) H$_3$B·NMeH$_2$ oligomerization;[42] (b) H$_3$B·PPh$_2$H oligomerization;[45,47] (c) B−B homocoupling.[50]

Scheme 4. Formation of Rh(I) and Rh(III) Starting Materials[a]
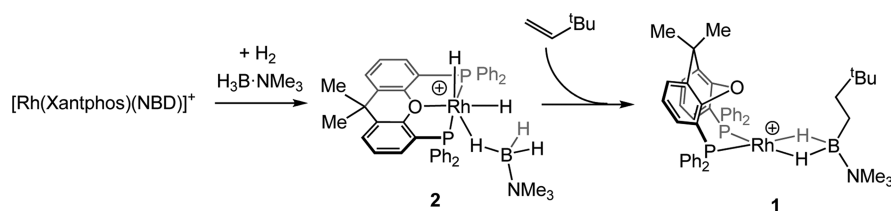
[a]See ref 50. [BAr$^F_4$]$^-$ anions are not shown. 1,2-F$_2$C$_6$H$_4$ is the solvent.

hydrogen redistribution reactions can also occur, in which amino−boranes take part in hydrogen transfer with amine−boranes,[34,39] while a nucleophilic solvent (e.g., THF) can also potentially catalyze polyaminoborane formation from amino−boranes.[40]

Mechanistic insight that comes from the direct observation of intermediates in dehydropolymerization is also very rare, although off-cycle products have been reported.[13,29,41] The product of the first insertion event of H$_3$B·NMeH$_2$ using the [Ir(PCy$_3$)$_2$(H)$_2$]$^+$ fragment has been shown to be [Ir-(PCy$_3$)$_2$(H)$_2$(η^2-H$_3$B·NMeHBH$_2$·NMeH$_2$)][BAr$^F_4$] [Ar^F = 3,5-(CF$_3$)$_2$C$_6$H$_3$],[42] in which the resulting diborazane forms a σ[43] complex with the Ir center (Scheme 3a). Studies on closely related phosphine−borane dehydrocoupling[44] using the [Rh-(Ph$_2$P(CH$_2$)$_3$PPh$_2$)]$^+$ fragment, which is also an excellent catalyst for amine−borane dehydropolymerization,[21] provide complementary insight, and intermediates that sit each side of the dehydrocoupling step have been characterized, allowing for activation parameters for the P−B bond forming event to be determined (Scheme 3b).[45−47] These intermediates show that P−H activation has occurred to give a Rh(III) phosphino hydride with supporting intra- and intermolecular σ (B−H··· Rh) interactions. By using the [Rh(Xantphos)]$^+$ fragment (Xantphos = 4,5-bis(diphenylphosphino)-9,9-dimethylxan-thene),[48,49] which is valence isoelectronic to [Ir-(^{t}BuPOCOP^{t}Bu)],[15,34] B−B homocoupling of H$_3$B·NMe$_3$ gives a diborane(4) complex (Scheme 3c). Computation and

experiment point to a pathway in which a low energy reversible B−H activation of amine−borane is followed by a second, higher energy B−H activation and B−B coupling,[50] with these steps being related to those generally invoked in B−N bond formation in dehydropolymerization.

Encouraged by the ability of the [Rh(Xantphos)]$^+$ fragment to B−B homocouple amine−boranes, we now report its use in a detailed stoichiometric, catalytic, and mechanistic/kinetic investigation into the dehydropolymerization of H$_3$B·NMeH$_2$ to form polyaminoborane. Additional mechanistic and structural data on the processes occurring comes from the reactions of this fragment with H$_3$B·NMe$_3$, H$_2$B═N^{i}Pr$_2$, and H$_3$B·NMe$_2$H. These studies lead to an overall mechanistic framework for dehydropolymerization using transition-metal fragments that supports and adds to the dehydrogenation/ coordination/insertion mechanism proposed by others.[15,22,23,28,37] This insight leads to the gross control of the degree of dehydropolymerization, allowing for both low- and higher-molecular-weight polyaminoboranes to be obtained.

2. RESULTS

2.1. Stoichiometric Reactivity of Precatalyst [Rh(κ^2-$_{PP}$-Xantphos)(η^2-H$_2$B(NMe$_3$)CH$_2$CH$_2$^{t}Bu)][BAr$^F_4$]. 2.1.1. H$_3$B·NMe$_3$. The stoichiometric reactivity of the [Rh(Xantphos)]$^+$ fragment with amine−boranes is described first, as this provides baseline reactivity with which to contextualize subsequent

Scheme 5. Reactivity of 2^a
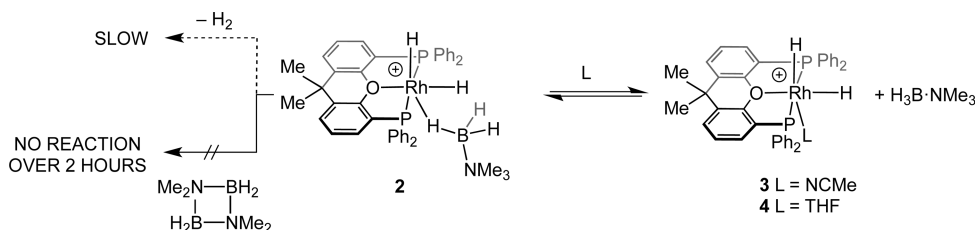
^{a}[BAr$^F_4$]$^-$ anions are not shown. 1,2-F$_2$C$_6$H$_4$ is the solvent.

Scheme 6. Dehydrocoupling of H$_3$B·NMe$_2$H^a
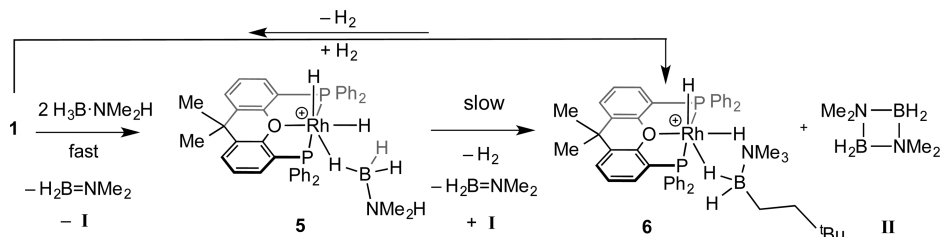
^{a}[BAr$^F_4$]$^-$ anions are not shown. C$_6$H$_5$F is the solvent.

catalytic studies. Many of our previous investigations into the coordination, reaction, and catalytic chemistry of amine and phosphine−boranes with cationic Rh(I) fragments have used [Rh(L)$_2$(η-arene)][BAr$^F_4$] (L = phosphine; arene = C$_6$H$_5$F or 1,2-F$_2$C$_6$H$_4$) precursors as a convenient latent source of the {Rh(L)$_2$}$^+$ fragment, with these being formed from hydrogenation of the corresponding NBD (norbornadiene) adduct in fluorobenzene or 1,2-difluorobenzene solvents.[21,45,51,52] Surprisingly, in these solvents, we have not been able to make the corresponding Rh(I)−Xantphos fluoroarene precatalyst, as decomposition to as yet unidentified product(s) occurs. Thus, we turned to the previously reported and structurally characterized[50] Rh(I) species [Rh(κ^2-$_{PP}$-Xantphos)(η^2-H$_2$B-(NMe$_3$)CH$_2$CH$_2$^{t}Bu)][BAr$^F_4$], **1**, and the Rh(III) complex [Rh(κ^3-$_{POP}$-Xantphos)(H)$_2$(η^1-H$_3$B·NMe$_3$)][BAr$^F_4$], **2**, as reliable and relatively stable [Rh(Xantphos)]$^+$ precatalysts (Scheme 4). Complex **1** has the hydroborated alkene H$_2$B(NMe$_3$)CH$_2$CH$_2$^{t}Bu, **I**, ligated to the metal center through two Rh···H−B σ interactions, while **2** has a H$_3$B·NMe$_3$ bound through a single Rh···H−B interaction. These complexes also demonstrate the variability in the Xantphos coordination mode, mer-κ^3-POP and cis-κ^2-PP,[53,54] and are also related to recently reported cationic[53,55] and neutral[56,57] rhodium dihydride complexes with Xantphos-type ligands.

In solution under an Ar atmosphere, complex **2** forms as yet unidentified products (Scheme 5, 50% in 24 h), while under an H$_2$ atmosphere, it is stable showing no change after 24 h. These observations suggest that irreversible H$_2$ loss from **2** on the time scale of catalysis (∼90 min, vide infra) is slow. Addition of the dimeric amino−borane [H$_2$B−NMe$_2$]$_2$, **II**, to **2**, which has previously been shown to promote H$_2$ loss from other Rh(III) dihydride species,[27,58] resulted in no significant H$_2$ loss over the course of a few hours, although over 24 h, a new species becomes dominant that results from the reaction of H$_2$B═NMe$_2$, **II**, with **2** (see Section 2.2.9). Addition of excess NCMe to **2** forms the previously reported NCMe adduct **3**[55] and free H$_3$B·NMe$_3$, while addition of excess THF forms a (45:55) mixture of **2** and a complex spectroscopically characterized as the THF adduct: [Rh(κ^3-$_{POP}$-Xantphos)(H)$_2$(THF)][BAr$^F_4$], **4**

(Scheme 5).[59] Complex **4** also shows very similar NMR data to the analogous acetone adduct: [Rh(κ^3-$_{POP}$-Xantphos)-(H)$_2$(acetone)][BAr$^F_4$].[55] THF and H$_3$B·NMe$_3$ binding are thus competitive. Although irreversible H$_2$ loss is proposed to be slow, H/D exchange at Rh−H and B−D is shown to be rapid (on time of mixing) by ^{1}H and ^{2}H NMR spectroscopy when [Rh(κ^3-$_{POP}$-Xantphos)(H)$_2$(η^1-D$_3$B·NMe$_3$)][BAr$^F_4$], d_3-**2**, is generated in situ by addition of H$_2$ to a 1:1 mixture of [Rh(κ^2-$_{PP}$-Xantphos)(NBD)][BAr$^F_4$] and D$_3$B·NMe$_3$. Presumably this occurs via B−H activation at the Rh(III) dihydride fragment, via a σ-CAM mechanism (σ-complex-assisted metathesis),[60] to give a base-stabilized dihydrogen−boryl species[61−64] that can then reform to give an alternative isotopomer. However, any equilibria operating must sit far to the side of **2** as there is no evidence by NMR spectroscopy for the formation of a new species when **2** is placed under H$_2$ (4 atm). Addition of H$_3$B·NMe$_3$ to **1** results in the slow formation of the corresponding diborane(4) complex (Scheme 3c) that comes from sequential B−H activation of two amine−boranes.[50]

2.1.2. H$_3$B·NMe$_2$H. Addition of 2 equiv of H$_3$B·NMe$_2$H to **1** results in the immediate (time of mixing) generation of the analogous complex to **2**, [Rh(κ^3-$_{POP}$-Xantphos)(H)$_2$(η^1-H$_3$B·NMe$_2$H)][BAr$^F_4$], **5**, alongside free H$_2$B(NMe$_3$)CH$_2$CH$_2$^{t}Bu, **I** (Scheme 6). Complex **5** has been characterized by NMR spectroscopy by analogy with **2** (Supporting Information) and other σ borane complexes.[65] In particular, in the ^{1}H NMR spectrum, relative integral 1 H signals are observed at δ −14.11 (br) and δ −19.05 (doublet of triplet of doublets) for the inequivalent Rh−hydrides, and a broad integral 3 H signal at δ −1.31 is assigned to the σ-bound H$_3$B·NMe$_2$H Rh···H−B groups that are interconverting between bridging and terminal positions.[43,61] The ^{31}P{^{1}H} NMR spectrum shows a single environment at δ 44.5 [J(RhP) = 115 Hz], while the ^{11}B NMR spectrum shows a broad signal at δ −12, barely shifted from free H$_3$B·NMe$_2$H (δ −12.8), consistent with an η^1-coordination of the amine−borane.[51] The amino−borane H$_2$B═NMe$_2$ and its consequent dimer [H$_2$B−NMe$_2$]$_2$, **II**,[66] are also formed, which arise from dehydrogenation of H$_3$B·NMe$_2$H with

concomitant transfer of H_2 to Rh. Complex **5** is not stable and is slowly consumed, so that after 5 h, the Rh(III) dihydride $[Rh(\kappa^3{-}_{POP}{-}Xantphos)(H)_2(\eta^1{-}H_2B(NMe_3)CH_2CH_2{}^tBu)]{-}[BAr^F_4]$ **6** is formed alongside $[H_2B{-}NMe_2]_2$ (Scheme 6). Complex **6** has been spectroscopically characterized (see the Supporting Information) and shows very similar data to **2** and **5** but now has the borane **I** bound to the metal center. Complex **6** presumably forms after dehydrogenation of **5** (and release of H_2) in the absence of excess $H_3B{\cdot}NMe_2H$. Interestingly **1** and **6** are shown to be in equilibrium with one another, as addition of H_2 (4 atm) to **1** results in a 3:1 mixture of **6** to **1**, which is biased back in favor of **1** on removal of H_2. However, we discount a significant role for the equilibrium between **6** and **1** during catalysis, based on the following observations: (i) **1** rapidly reacts with $H_3B{\cdot}NMe_2H$ to form **5**; (ii) **6** only forms slowly at low $H_3B{\cdot}NMe_2H$ concentration from **5**; (iii) the temporal evolution of catalysis is the same whether starting from Rh(I) or Rh(III) precursors; and (iv) excess **I** does not change the observed temporal profile of catalysis (vide infra). This is contrast to the autocatalytic role that the final product $[H_2B{-}NMe_2]_2$ has been shown to take in dehydrocoupling of $H_3B{\cdot}NMe_2H$ as catalyzed by the $[Rh(PCy_3)_2(H)_2]^+$ fragment.[27] Addition of D_2 to **5**/$H_3B{\cdot}NMe_2H$ results in H/D exchange at the B–H and Rh–H positions as well as in the free amine–borane (as measured by ^2H NMR spectroscopy) indicating that reversible B–H activation is a relatively low energy process. No H/D exchange was observed at nitrogen (by ^2H NMR spectroscopy), suggesting that reversible N–H activation is considerably higher in energy, as has been noted before in related systems.[66,67] Slow dehydrogenation of $H_3B{\cdot}NMe_2H$ is also observed.

2.1.3. $H_3B{\cdot}NMeH_2$. Addition of 2 equiv of $H_3B{\cdot}NMeH_2$ to **1** resulted in the immediate formation of the Rh(III) dihydride complex $[Rh(\kappa^3{-}_{POP}{-}Xantphos)(H)_2(\eta^1{-}H_3B{\cdot}NMeH_2)][BAr^F_4]$, **7** (Scheme 7). Complex **7** was characterized by NMR

Scheme 7. Borazine Formation at Low $[H_3B{\cdot}NMeH_2]^a$
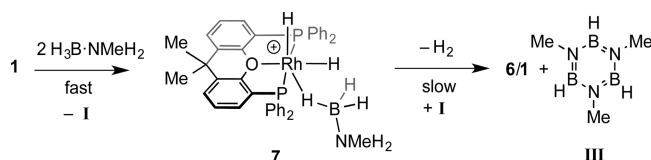
$^a[BAr^F_4]^-$ anions are not shown. C_6H_5F is the solvent.

spectroscopy, and these data are very similar to those for **2**, **5**, and **6**. The amino–borane that would arise from initial dehydrogenation, $H_2B{=}NMeH$, was not observed;[38] however, the ultimate thermodynamic product of dehydrocoupling, *N*-trimethylborazine, **III**, was formed ($\delta(^{11}B)$ 33.3, doublet; lit. δ 33.2[68]). There was no evidence for the formation of polymeric BN materials or the potential cyclic triborazane intermediate, $[H_2BNMeH]_3$.[69] We have recently[39a] shown that when the amino–borane $H_2B{=}NH^tBu$ is released from a metal center it undergoes trimerization to form $[HBN^tBu]_3$ by an (unresolved) mechanism in which hydrogen-redistribution processes are occurring,[34] and it is possible that such processes are also operating here. As found for **5**, complex **7** undergoes a second, slower dehydrogenation. This process is a little faster than for **5**, taking 2 h to fully consume **7** to afford **III** and an equilibrium mixture of **6/1**. Addition of NCMe (excess) to **7** affords the corresponding MeCN adduct, **3**, and free $H_3B{\cdot}NMeH_2$.

2.1.4. General Comments on the Stoichiometric Reactivity. These observations show that, under noncatalytic conditions, dehydrogenation of $H_3B{\cdot}NMe_2H$ or $H_3B{\cdot}NMeH_2$ at a Rh(I) center (i.e., **1**) is rapid, while at a Rh(III) dihydride center (i.e., **5** or **7**), it is slower, even though B–H activation (as measured by H/D exchange experiments for $H_3B{\cdot}NMe_3$) is fast at the RhH_2 center. These observations are similar to those previously reported for the $[Rh(PR_3)_2]^+$ and $[Rh(PR_3)_2(H)_2]^+$ fragments, respectively.[27,51] As will be demonstrated, this slower rate of dehydrogenation of **5** and **7** is in contrast to the fast consumption of $H_3B{\cdot}NMe_2H$ or $H_3B{\cdot}NMeH_2$ under catalytic conditions (e.g., 0.2 mol % **1**, 0.072 M $H_3B{\cdot}NMe_2H$). In addition, under catalytic conditions, $H_3B{\cdot}NMeH_2$ is dehydropolymerized to give $[H_2BNMeH]_n$ rather than forming trimethylborazine **III**, and there is an induction period observed before catalysis. These observations suggest additional mechanistic considerations need to be adopted under the conditions of high ratios of amine–borane to metal–ligand fragment, and these are discussed next.

2.2. Catalysis. *2.2.1. Initial Experiments Using $H_3B{\cdot}NMe_2H$ and $H_3B{\cdot}NMeH_2$.* Under catalytic conditions (0.2 mol % **1**, 0.072 M $H_3B{\cdot}NMe_2H$, 1,2-$F_2C_6H_4$ as solvent, open system to a slow flow of Ar), complex **1** catalyzes the dehydrogenation of $H_3B{\cdot}NMe_2H$ to ultimately form dimeric **II** (Scheme 8a). Following this reaction by ^{11}B NMR spectroscopy using periodic sampling of the reaction mixture shows that there was an induction period of approximately 400–500 s, and $H_2B{=}NMe_2$ was also observed as an intermediate during the productive phase of catalysis. Turnover is relatively fast once the induction period is over, with an overall ToF $\sim$1200 h^{-1} (ToN = 500), which is a rate that is comparable to $[Rh(Ph_2PCH_2CH_2CH_2PPh_2)(\eta^6{-}C_6H_5F)][BAr^F_4]$,[21] which also shows an induction period and is suggested to be homogeneous in character. Very similar temporal profiles are observed starting from the Rh(III) complex **2** (Supporting Information), suggesting that the induction period is not due to the formation of the simple Rh(III) analogue (i.e., **5**), consistent with the rapid formation of **5** from **1** (Scheme 6). This also argues against the involvement of **I** during the induction period or catalysis, as **2** is generated without **I** being present. At $\sim$30% conversion ($\sim$900 s), addition of Hg to the catalyst solution, or filtration of the catalyst mixture though a 0.2 μm filter and addition of a further 500 equiv of $H_3B{\cdot}NMe_2H$, did not result in the termination of catalysis (see the Supporting Information): observations that suggest a homogeneous system.[54] The catalyst can also be recycled, in that addition of a further 500 equiv of $H_3B{\cdot}NMe_2H$ to the catalytic mixture directly at the end of catalysis resulted in essentially the same rate and overall turnover number. There is no induction period observed in this recharging experiment or in the filtration experiment, suggesting that the catalyst remains in its active form in both. No significant amount of the linear diborazane $H_3B{\cdot}NMe_2BH_2{\cdot}NMe_2H$[68] was observed, similar to $[Rh(Ph_2PCH_2CH_2CH_2PPh_2)(\eta^6{-}C_6H_5F)][BAr^F_4]$[21] but different from $[Rh(PR_3)_2H_2]^+$ systems where it is observed in significant amounts.[27,51,58]

In a closed system (New Era high pressure NMR tube), catalysis is significantly slower (Scheme 8b), with ToF $\sim$130 h^{-1} (ToN = 500). A very similar induction period to the open system is observed, and $H_2B{=}NMe_2$ is also an intermediate. We[27] and others[23] have commented previously on the rate inhibition by H_2 in amine–borane dehydrocoupling. For example, with the $[Rh(PCy_3)_2]^+$ catalyst, H_2 buildup forces

Scheme 8. ^{11}B Time/Concentration Plots of the Dehydrocoupling of $H_3B \cdot NMe_2H^a$

(a)   Open System
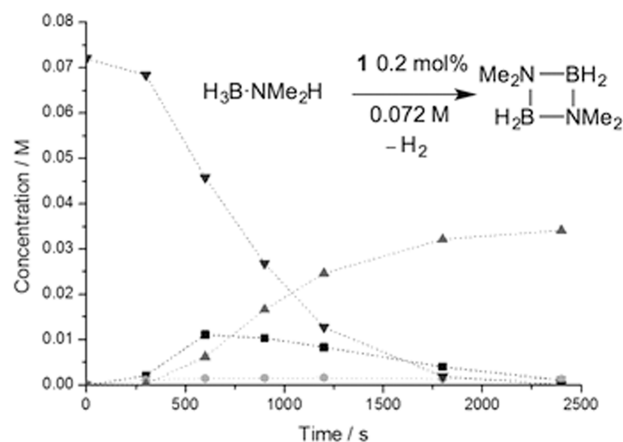
(b)   Closed System
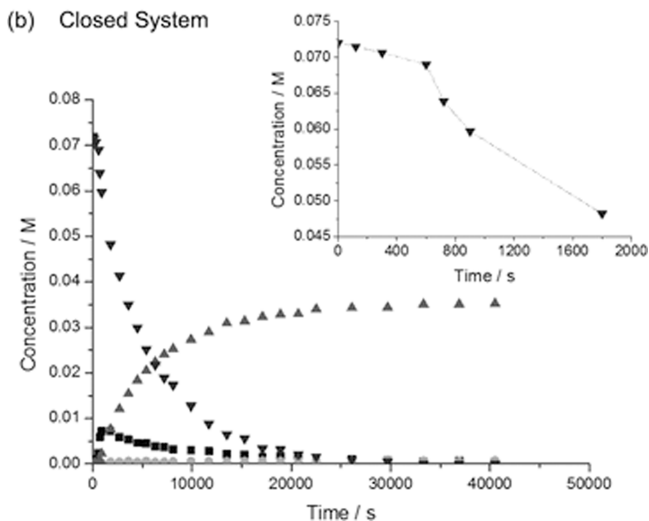
^{a} (▼) $H_3B \cdot NMe_2H$, (■) $H_2B{=}NMe_2$, (▲) $[H_2B{-}NMe_2]_2$, (●) $BH(NMe_2)_2$. 0.2 mol % **1**, [**1**] = 1.44×10^{-4}, 0.072 M $H_3B \cdot NMe_2H$, 1,2-$F_2C_6H_4$ is the solvent. (a) Open system; (b) closed system. Inset shows the induction period.

the system to sit in a Rh(III)/Rh(III) cycle that turns over considerably slower than the Rh(I)/Rh(III) cycle. The more active Rh(I) oxidation state is generated by addition of the product **II** to $[Rh(PCy_3)_2(H)_2]^+$ that promotes H_2 reductive elimination, i.e., autocatalysis. In our system, addition of 200 equiv of **II** prior to catalysis (0.2 mol % **1**, 0.072 M amine–borane, open system) resulted in no significant change in the reaction profile, consistent with the lack of reaction between **1** and **II** under stoichiometric conditions on the time scale of catalysis (Scheme 5). Addition of 55 equiv of **I** also did not change the catalytic temporal profile (Supporting Information) demonstrating that it does not act to modify catalysis.

Catalyst **1** also dehydropolymerizes $H_3B \cdot NMeH_2$ (0.2 mol % **1**, 0.44 M amine–borane, open system, 2 h, C_6H_5F as solvent) to afford polyaminoborane $[H_2BNMeH]_n$ (M_n = 22 700 g mol^{-1}, PDI = 2.1 using polystyrene standards for GPC column calibration). This is lower molecular weight than typically formed using the $[Ir(^tBuPOCOP^tBu)H_2]$ catalyst (M_n = 55 200 g mol^{-1}, PDI = 2.9) in THF as solvent.[15] The Rh(III) catalyst **2**

also produced a very similar polymer to that for **1** (M_n = 24 800 g mol^{-1}, PDI = 1.9). These polymers formed show ^{11}B NMR spectra very similar to that reported for high-molecular-weight $[H_2BNMeH]_n$ produced from $[Ir(^tBuPOCOP^tBu)H_2]^{17}$ and $[Rh(Ph_2PCH_2CH_2CH_2PPh_2)(\eta^6{-}C_6H_5F)][BAr^F_4]^{21}$ catalysts, with a broad, symmetrical peak observed at δ −5.4 (fwhm = 720 Hz, Figure 1a).[15] No significant signals were observed

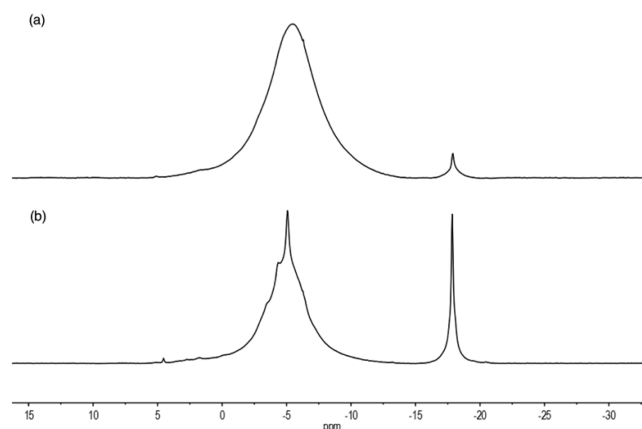**Figure 1.** (a) ^{11}B{^{1}H} NMR spectrum of the material that is isolated after dehydropolymerization of $H_3B \cdot NMeH_2$ using **1** (0.2 mol % 0.44 M $H_3B \cdot NMeH_2$, open system, 2 h). The signal at δ −17 is assigned to entrained $H_3B \cdot NMeH_2$ that reduces significantly in relative intensity on addition of more **1** (0.2 mol %, Supporting Information). (b) Under sealed conditions (H_2 build up). The signals at $\sim\delta$ 5 and $\sim\delta$ −17 split into a triplet and quartet, respectively (Supporting Information), reminiscent of the signals observed for $H_3B \cdot NMeHBH_2 \cdot NMeH_2$,[42] suggesting the presence of short-chain oligomers.

around δ 0 that might indicate chain branching,[23] although such a feature if small could be lost in the peak width of the main signal. To the detection limit of ^{11}B NMR spectroscopy (ca. 5%), no signals were observed between δ 30−40 that could be assigned to free MeHN$=$BH(R).

A time/conversion plot for $H_3B \cdot NMeH_2$ dehydrocoupling to form polyaminoborane using catalyst **1** in an open system is shown in Scheme 9 alongside a hydrogen-evolution plot, as measured by gas buret. As for $H_3B \cdot NMe_2H$, there is a significant induction period (10 min) before the rapid dehydrocoupling occurs. Polymer formation and hydrogen evolution track one another, and by the end of catalysis (7200 s, 98% conversion, ToF $\sim$250 h^{-1}), just over 1 equiv of H_2 has been produced, consistent with the formation of polyamino-borane of empirical formula approximating to $[H_2BNMeH]_n$. This reaction is considerably slower than for $H_3B \cdot NMe_2H$, but this might reflect the poorer solubility of $H_3B \cdot NMeH_2$ in C_6H_5F. Neither trimethylborazine, **III**, nor signals assignable to free $H_2B{=}NMeH$ were observed during the reaction using ^{11}B NMR spectroscopy when interrogated by regular sampling of the catalysis mixture.

Addition of the linear diborazane $H_3B \cdot NMeHBH_2 \cdot NMeH_2$[68] to **1** (20 mol %) in a sealed NMR tube resulted in the formation of N−trimethylborazine **III**, alongside unidentified metal products. No significant amounts of polyaminoborane or cyclic triborazane $[MeHNBH_2]_3$[69] were observed under these near-stoichiometric conditions. However, at 0.4 mol % of **1** significant amounts of polyaminoborane were observed (M_n = 15 400 g mol^{-1}, M_w = 27 800 g mol^{-1}, PDI = 1.8), so that this is

Scheme 9. Polymer Conversion Plot (Triangles) and H$_2$ Evolution (Squares, Gas Buret, Calculated at 26 °C) for the Dehydrocoupling of H$_3$B·NMeH$_2$^{a}
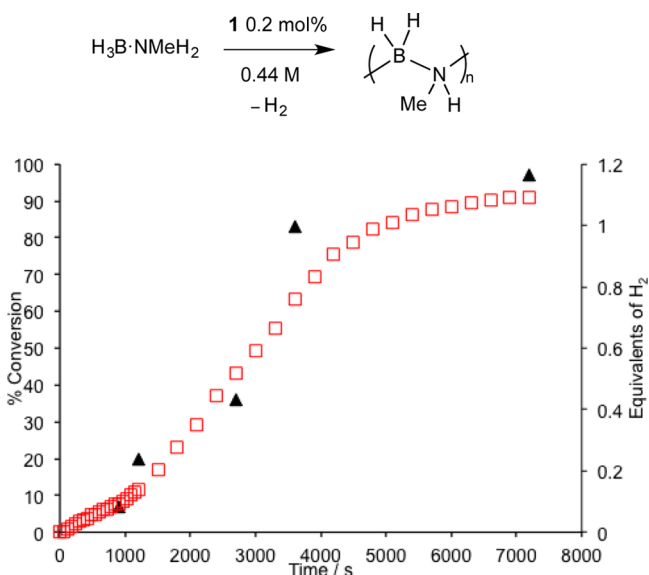
^{a}For polymer conversion, each point is a separate experiment in C$_6$H$_5$F, with the product precipitated with hexane. The conversion of H$_3$B·NMeH$_2$ (δ −17.8) relative to [H$_2$BNMeH]$_n$ (δ −5.4, br) measured by ^{11}B{^{1}H} NMR spectroscopy (THF solvent).

now the major species formed (~90% by ^{11}B NMR spectroscopy, Scheme 10). This process presumably occurs

Scheme 10. Redistribution Reactions^a

both observed at 0.4 mol% (~ 10:1)
no polyaminoborane observed at 20 mol%
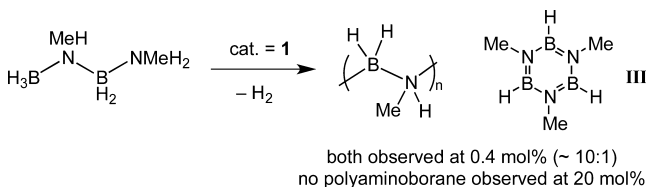
^{a}Closed system: [**1**] = 0.4 mol %, [H$_3$B·NMeHBH$_2$·NMeH$_2$] = 0.22 M. Open system: [**1**] = 20 mol %, [H$_3$B·NMeHBH$_2$·NMeH$_2$] = 0.11 M.

via metal-promoted B−N bond cleavage, possibly via a Rh σ amine−borane intermediate,[27,51] to give H$_2$B═NMeH and H$_3$B·NMeH$_2$, which both proceed under the appropriate conditions of substrate concentration to give polyaminoborane and/or **III**. The formation of only **III** at low substrate

concentration is consistent with the stoichiometric experiments using H$_3$B·NMeH$_2$ (i.e., Scheme 7). A very similar redistribution of H$_3$B·NMeHBH$_2$·NMeH$_2$ to afford poly-(methylaminoborane) has been reported using the [Ir-(^{t}BuPOCOP^{t}Bu)H$_2$] catalyst,[34] which is also suggested to operate via B−N bond cleavage and an amino−borane intermediate, although this catalyst produces polyaminoborane of higher M_n (67 400 g mol$^{−1}$, PDI = 1.4) under the conditions used. Ru(PNP)(H)(PMe$_3$)-based systems have also been shown, by cyclohexene trapping experiments, to promote redistribution of polyaminoborane.[23] Addition of the secondary linear diborazane H$_3$B·NMe$_2$BH$_2$·NMe$_2$H to **1** (20 mol %) in a sealed NMR tube ultimately formed [H$_2$B−NMe$_2$]$_2$ after 24 h. After 100 min of reaction, 55% of the linear diborazane had been consumed, with H$_2$B−NMe$_2$, [H$_2$B═NMe$_2$]$_2$, boranediamine HB(NMe$_2$)$_2$,[70] and the amidodiborane (H$_2$B)$_2$(μ-H)(NMe$_2$)[34] all being observed in significant amounts. These last two species suggest B−N bond cleavage is occurring to form free NMe$_2$H, as has been explored computationally and kinetically in thermal rearrangements of linear diborazanes.[34] That both primary and secondary linear diborazanes react with complex **1** to ultimately form the final products of dehydrocoupling shows that, although they are not observed during catalysis, their formation, either transiently metal-bound or free, cannot be discounted.

2.2.2. Effect of Solvent on Polymerization. Changing the solvent to THF produced polyaminoborane (catalyst = **1**, 0.2 mol %) with higher molecular weight (M_n = 52 200 versus 22 700 g mol$^{−1}$) than for C$_6$H$_5$F solvent but now taking a significantly longer time to reach near completion (19 h versus 2 h, Table 1). This suggests THF slows the rate of dehydropolymerization, possibly by the reversible formation of an adduct (cf., **4**), and this may also have a role to play in attenuating any chain termination events if competitive with H$_2$ binding[71] (see below). Alternatively, more of the catalyst could sit as the simple adduct species **4** leading to fewer active metal sites and thus longer polymer chains growing from the metal. THF may also solvate the growing polymer better leading to longer chain growing from the metal. Only a very small quantity of trimethylborazine, **III**, was observed (1−2%). THF solvent might also result in a change in mechanism to one which involves hydride donation to the metal to form a THF-stabilized borenium, that is, [(NMeH$_2$)(THF)BH$_2$]$^+$.[32]

2.2.3. Polymer Growth Kinetics and Control over Molecular Weight Using Hydrogen. A plot of number-averaged degree of polymerization, DP$_n$ (DP$_n$ = M_n/ M(H$_2$B═NMeH)) versus conversion for the dehydrocoupling of H$_3$B·NMeH$_2$ using **1** (0.2 mol %, open system) shows a

Table 1. Dehydropolymerization Data, M_n by GPC^a

entry	condition	M_n (g mol$^{−1}$)	PDI
1	**1**, 0.2 mol %	22 700	2.1
2	**2**, 0.2 mol %	24 800	1.9
3	**1**, 0.4 mol %, 0.22 M, H$_3$B·NMeHBH$_2$·NMeH$_2$	15 400	1.8
4	**1**, 0.2 mol %, further 500 equiv	17 900	1.8
5	**1**, 1 mol %	7 500	1.5
6	**1**, 0.2 mol %, closed	2 800	1.8^b
7	**1**, 0.2 mol %, THF solvent	52 200	1.4^c
9	**1**, 0.2 mol %, excess cyclohexene	38 600	1.8

^{a}100% conversion after first measured point (2 h) as determined by ^{11}B NMR spectroscopy. 0.44 M [H$_3$B·NMeH$_2$], open system, C$_6$H$_5$F unless otherwise stated. ^{b}Greater than 95% conversion, 24 h. ^{c}85% conversion, 19 h.

relationship that is suggestive of a predominately chain-growth mechanism for the growing polymer (Scheme 11). Such a

Scheme 11. (a) Degree of Polymerization versus Conversion;[a](b) Addition of a Further 500 equiv of H₃B·NMeH₂ to 1 after Catalysis; (c) Control over Molecular Weight Using H₂ (C₆H₅F Solvent) or THF Solvent
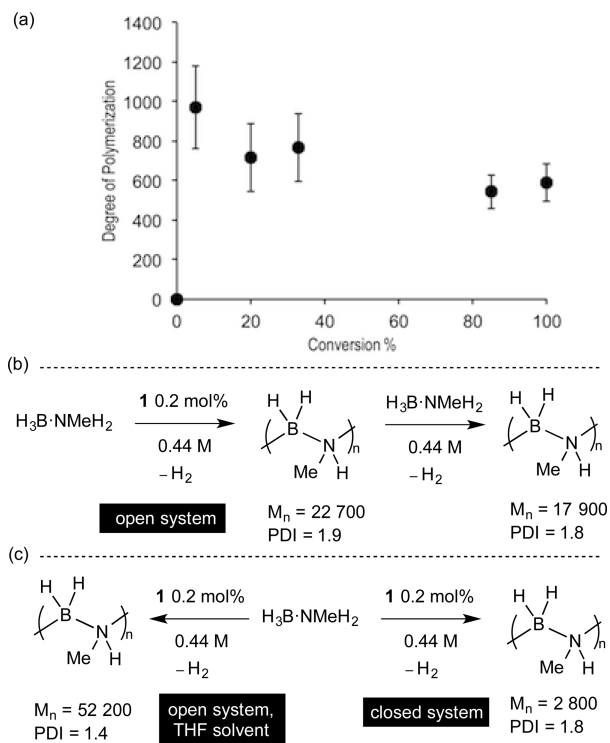
[a]0.2 mol % **1**, 0.44 M [H₃B·NMeH₂], open system. Each point is a separate experiment in C₆H₅F with varying time, with the product precipitated with hexanes. Degree of polymerization determined by GPC. Polymer conversion measured by $^{11}B\{^1H\}$ NMR spectroscopy. Data points come from three repeat analyses on the same sample, with the mean value and standard error shown.

process has been proposed previously for the [Ir-(tBuPOCOP'Bu)H₂] catalyst system for which a modified chain-growth mechanism is invoked, in which slow dehydrogenation to form amino−borane is followed by faster metal-mediated polymerization of this unsaturated fragment.[15] This suggestion is on the basis of the polymer conversion kinetics that show that high-molecular-weight polymers are present at low (less than 40%) conversion, coupled with the observation that higher catalyst loadings lead to higher-molecular-weight polymer. A similar mechanism has been proposed for the dehydropolymerization of ammonia−borane using bifunctional Ru catalysts.[23] Our polymer conversion kinetics suggest a similar mechanism is operating, in that there is a high degree of polymerization at low conversion (M_n = 30 800 g mol⁻¹, PDI = 1.4 at 20% conversion; M_n = 25 300 g mol⁻¹, PDI = 1.6 at 100% conversion).[72] However, in contrast to the [Ir(tBuPOCOP'Bu)-H₂] systems, when the catalyst loading is increased (i.e., ×5 the loading, 1 mol %), the polymer that results is now of significantly lower molecular weight but similar polydispersity (M_n = 7500 g mol⁻¹, PDI = 1.5). This strongly suggests a metal-centered process, as initially proposed by Baker and Dixon for the catalytic dehydrogenation of ammonia−borane.[37] $^{11}B\{^1H\}$ NMR data for each conversion point show broadly

similar peak profiles centered around δ −5. In particular, those at low conversions and high conversions are qualitatively the same, suggesting the nature of the polymer in each is similar.

Addition of a further 500 equiv of H₃B·NMeH₂ to a reaction postpolymerization resulted in further dehydropolymerization, to yield polymer with similar molecular weight and polydispersity to before (M_n = 17 900 g mol⁻¹, PDI = 1.8), over a similar time scale. This result shows that the catalyst remains active directly after catalysis has finished but it is not a living system and there must be some chain transfer/termination process occurring.

In a closed system (Youngs flask, ~30 cm³ volume, stirred), dehydropolymerization also proceeds essentially to completion (Scheme 11, Table 1) but over a much longer time scale than in an open system (24 h versus 2 h) The resulting isolated solid is waxy in appearance, suggesting a lower M_n polymer compared with the free-flowing solid produced in an open system. A $^{11}B\{^1H\}$ NMR spectrum of this material shows a broad, poorly resolved peak centered around δ −5 that also shows evidence for shorter-chain oligomeric species, compare H₃B·NMeHBH₂·NMeH₂,[34,42] by an overlaid sharper signal that becomes a broad triplet in the ^{11}B NMR spectrum (Figure 1b). There is also a smaller intensity signal ~δ −18 in the region associated with BH₃ groups,[29] which is also coincident with residual H₃B·NMeH₂. Analysis of this material by GPC showed that the polymer produced under these conditions of exogenous hydrogen was considerably shorter than that produced in an open system (M_n = 2800 g mol⁻¹, PDI = 1.8). This demonstrates that hydrogen potentially acts as a modifier in the catalytic process, and we suggest it acts as a chain transfer reagent, as in Ziegler−Natta ethene polymerization where hydrogen can used control polymer molecular weight.[1,73]

2.2.4. Probing Free H₂B═NMeH as an Intermediate. As discussed in the Introduction, the hydroboration of exogenous cyclohexene has previously been shown to act as a marker for the presence of free amino−borane H₂B═NMeH in dehydropolymerization reactions.[22,34,37] In the presence of cyclohexene using 50 mol % of **1** with H₃B·NMeH₂, the hydroborated product Cy₂B═NMeH is observed as the major boron-containing product, alongside **III** as the minor product (Scheme 12). This suggests that, at low substrate concentration, free amino−borane is generated, which has sufficient lifetime for reaction with cyclohexene. By contrast, at high substrate concentrations (0.2 mol % **1**), no hydroborated product is observed. Instead, polymer is produced, interestingly with a significantly higher molecular weight than formed in the

Scheme 12. Cyclohexene Trapping Experiments[a]
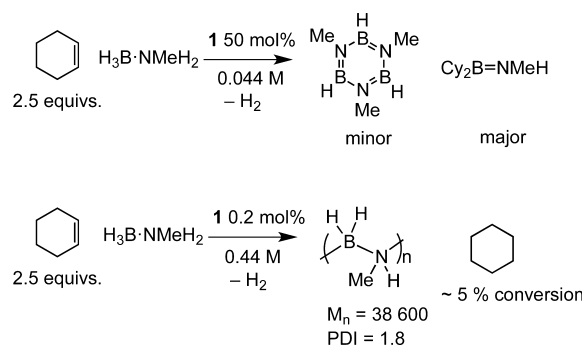
[a]Solvent = C₆H₅F.

absence of cyclohexene (M_n = 38 600 g mol^{-1}, PDI = 1.8). A small amount of cyclohexane is also formed (~5% conversion). This suggests that, under this concentration regime, free amino–borane is not produced in concentrations that allow for hydroboration of cyclohexene. As **2** has been reported to reduce cyclohexene to cyclohexane while becoming a Rh(I) species,[50] the longer polymer chain length could be a result of a lower concentration of the Rh(III) precatalyst (e.g., **7**), which would concomitantly result in fewer active sites for polymerization. Alternatively, cyclohexene could simply attenuate chain transfer by being competitive with H$_2$ for binding to the active catalyst (vide infra).

2.2.5. Kinetic Studies on H$_3$B·NMe$_2$H: Open System. The low solubilities of H$_3$B·NMeH$_2$ and the resulting polyamino-borane preclude detailed solution-based kinetic investigations. We have thus conducted more detailed studies on the catalytic process occurring using soluble H$_3$B·NMe$_2$H, which ultimately dehydrogenates to give **II**. That both primary and secondary amine–borane systems show very similar reaction profiles (induction period, same binding mode and reactivity with the {Rh(Xantphos)H$_2$}$^+$ fragment) suggests that this approximation is a reasonable one.

Following the temporal evolution of the dehydrocoupling of H$_3$B·NMe$_2$H in an open system (i.e., under a slow flow of Ar) under different substrate concentration regimes (0.018–0.288 M[74]) while keeping the concentration of **1** constant (1.44 × 10^{-4} M, i.e., 0.2 mol % at [H$_3$B·NMe$_2$H] = 0.072 M) led to the concentration/time plots as exemplified in Scheme 13 (also Supporting Information and Scheme 8a). All of these plots show very similar induction periods (~400 s) and the formation of H$_2$B=NMe$_2$ as an intermediate. At higher H$_3$B·NMe$_2$H concentration, that is, 0.288 M, the rate of consumption of amine–borane after this induction period appears to be pseudo-zero-order initially, behavior that is less pronounced at lower concentrations. This might suggest that saturation kinetics[75] are operating in this system at high H$_3$B·NMe$_2$H concentrations. To confirm this, a plot of rate of H$_3$B·NMe$_2$H consumption at constant Rh concentration versus time for each data point, excluding the induction period, over the H$_3$B·NMe$_2$H concentration range 0.018–0.228 M (i.e., a 16-fold change in concentration) reveals that saturation kinetics become important at a H$_3$B·NMe$_2$H concentration of ~0.1 M, above which a pseudo-zero-order dependence is observed (Scheme 14). At lower H$_3$B·NMe$_2$H concentration, this is now a pseudo-first-order relationship. The catalysis is first order in Rh concentration for an initial H$_3$B·NMe$_2$H concentration of 0.072 M, when the loading was varied between 0.1, 0.2, and 0.4 mol %. Kinetic isotope effect (KIE) studies measured during the zero-order phase showed a small but significant effect for exchanging N–H for N–D (k_h/k_d = 2.1 ± 0.2) suggesting a primary KIE but little effect on exchanging B–H/B–D (k_h/k_d = 0.9 ± 0.1). The induction period observed at the start of catalysis is approximately twice as long for NH/ND replacement and shows no change for BH/BD exchange.[76] These results suggest that N–H bond breaking is involved in both the turnover-limiting step during catalysis and the induction process. The KIE for NH activation is lower than that reported for H$_3$B·NMe$_2$H dehydrocoupling using Rh-(PCy$_3$)$_2$(H)$_2$Cl (k_h/k_d = 5.3 ± 1.2)[67] or Cp$_2$Ti (3.6 ± 0.3),[28] as well as H$_3$B·NH$_3$ dehydrocoupling using bifunctional Ru-(HPNP)(H)$_2$(PMe$_3$) (HPNP = HN(CH$_2$CH$_2$P^{t}Bu$_2$)$_2$) (5.3),[23] but is comparable to that measured for the Ni(NHC)$_2$ system (2.3)[77] in which the NHC ligand is involved in N–H transfer,[78]

Scheme 13. Time Concentration Plots for Different H$_3$B·NMe$_2$H Concentrations Using 1 as a Catalyst[a]
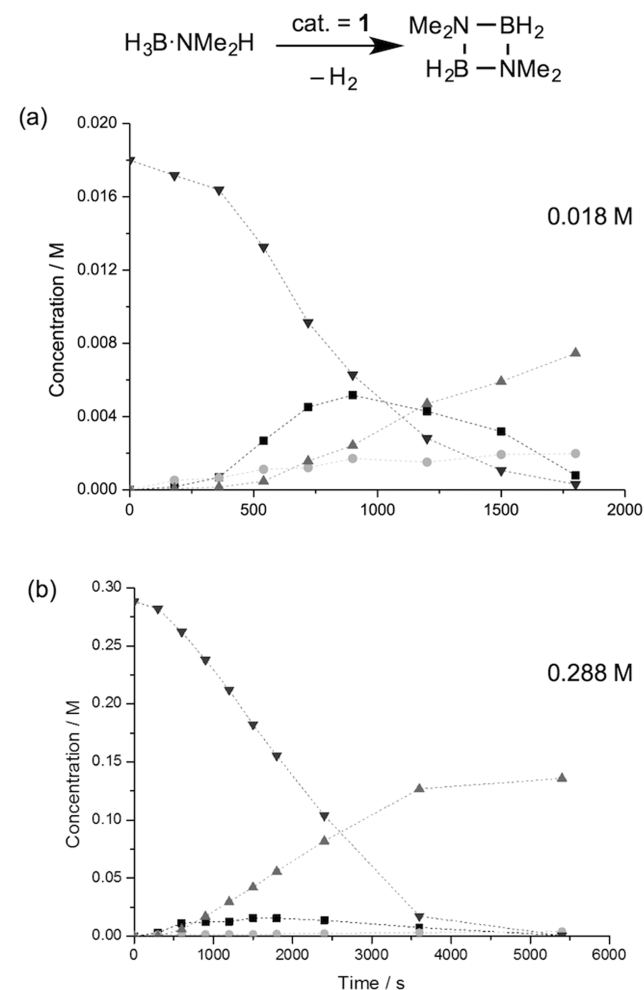
[a]Open system, 1,2-F$_2$C$_6$H$_4$, [**1**] = 1.44 × 10^{-4} M. (a) [H$_3$B·NMe$_2$H] = 0.018 M; (b) [H$_3$B·NMe$_2$H] = 0.288 M. Refer to Scheme 8a for [H$_3$B·NMe$_2$H] = 0.072 M. (▼) H$_3$B·NMe$_2$H, (■) H$_2$B=NMe$_2$, (▲) [H$_2$B−NMe$_2$]$_2$, (●) BH(NMe$_2$)$_2$.

and Shvo's catalyst (1.46 ± 0.9),[36] although in this last case, an H/D crossover mechanism was suggested to also operate that attenuates the observed KIE.

The postinduction period processes have been interrogated using a steady-state/saturation kinetics model that provides a good fit between observed and calculated rates (Scheme 14). In this model, the catalyst (**CAT**), produced via an induction process (k_{ind}, modeled but not further analyzed), binds H$_3$B·NMe$_2$H to form an intermediate (**CAT−AB**), which we propose has two amine–borane moieties (or derivatives thereof) bound. Ligation of two amine–boranes at a metal center has been observed experimentally,[52] suggested from kinetic models in Cp$_2$Ti dehydrocoupling catalysts,[28] and explored computationally.[79,80] At H$_3$B·NMe$_2$H concentrations above approximately 0.2 M, the turnover-limiting step occurs after the formation of **CAT−AB**, with the equilibrium between **CAT** and **CAT−AB**, if present, being strongly toward the latter.

2.2.6. Kinetic Studies on H$_3$B·NMe$_2$H: Closed System. As demonstrated by Scheme 8, performing the catalysis in a sealed NMR tube (0.2 mol % **1**, [H$_3$B·NMe$_2$H] = 0.072 M) leads to a considerably longer time for completion of catalysis. Interest-

Scheme 14. (a) Approximate Rate of [H₃B·NMe₂H] Consumption as a Function of Its Concentration, in an Open System Where [Rh]ₜₒₜ = 1.44 × 10⁻⁴ M, Based on Change in Concentration between Successive Data Pairs, after the Induction Phase, in Concentration−Time Data; (b) Experimental Concentration−Time Data for the Same Process, together with Data Simulated via the Model Indicated (Dotted Lines), where $k_2 = k_f = 0.72$ s⁻¹ and $(k_{-1} + k_2)/k_1 = K_m = 0.02$ Mᵃ

(a)

(b)
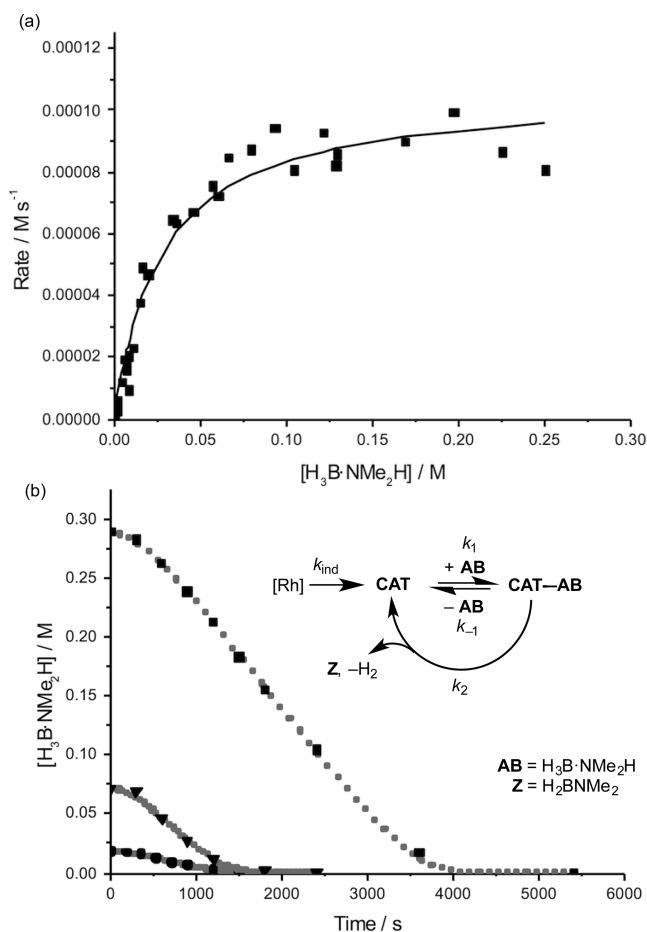
ᵃThe solid line is a Michaelis−Menten steady-state fitted by nonlinear regression, where K_m = 0.03 M and k_f = 0.74 s⁻¹. The k_{ind} value varied between the runs in the range 0.8−2.8 × 10⁻³ s⁻¹.

ingly, the consumption of H₃B·NMe₂H follows a first-order decay, postinduction period, over the whole of the reaction; k_{obs} = (4.13 ± 0.02) × 10⁻⁴ s⁻¹. Addition of a further 200 equiv of H₃B·NMe₂H to the closed system restarted catalysis at a rate and ToN that demonstrated that the majority of the catalyst remained active. Degassing the solution during catalysis in a sealed system also resulted in an immediate increase in the

relative rate of consumption of H₃B·NMe₂H (Supporting Information) suggesting that hydrogen acts to reversibly modify the active catalyst, possibly by forming a dihydrogen adduct, as discussed below.

2.2.7. Kinetic Studies on H₃B·NMeH₂: Open System. In an open system, a plot of rate of H₂ evolution, excluding the induction period, at an initial H₃B·NMeH₂ concentration of 0.44 M and 0.2 mol % **1**, reveals a temporal profile fully consistent with saturation kinetics, as also found for H₃B·NMeH₂. At concentrations of H₃B·NMe₂H below 0.1 M, pseudo-first-order kinetics are observed, while above 0.1 M, there is a pseudo-zero-order dependence (Supporting Information). These observations strengthen the likely similarities in the overall mechanism between H₃B·NMeH₂ and H₃B·NMe₂H.

2.2.8. Resting State during Catalysis: Evidence for an Amido−Borane Species? As our standard conditions of catalysis use only 0.2 mol % loadings of **1**, the observation of resting states (i.e., **CAT−AB**) is difficult by NMR spectroscopy. However, by using 5 mol % **1** in a sealed system, the temporal evolution of the catalyst can be monitored adequately using both ¹H and ³¹P{¹H} NMR spectroscopies. On addition of H₃B·NMe₂H to **1**, there is the immediate formation of **5** and a number of new species that we have been unable to assign definitively, although these appear to contain Rh−H moieties. Over time (3 h, 65% conversion of H₃B·NMe₂H), the NMR data show that, apart from **5**, one species is dominant. In the ¹H NMR spectrum, a broad multiplet is observed at δ −9.4, which sharpens on decoupling ¹¹B to reveal a doublet ($J(PH)$ 84 Hz) and a broad peak on ³¹P decoupling. These data suggest a B−H···Rh interaction *trans* to a phosphine. No corresponding Rh−H signal was observed. Broad peaks observed ∼δ −1.15 are suggestive of σ, Rh−H−B or Rh−H₂ interactions, but as this region overlaps with that in **5**, assignment is not definitive, and decoupling ¹¹B reveals no additional B−H signals over those for **5**. Inequivalent, poorly resolved phosphine environments, δ 23 ($J(RhP) \sim$ 160 Hz) and δ 4 ($J(RhP) \sim$ 120 Hz), are observed in the ³¹P{¹H} NMR spectrum. On the basis of these data, we *tentatively* assign a structure to this complex as the amido−borane⁸¹⁻⁸⁴ [Rh(κ²-ₚₚ-Xantphos)(H)(NMe₂BH₃)(L)][BArF₄], **8** (Scheme 15). The spectroscopic data do not allow us to comment on whether L = H₂ or H₃B·NMe₂H. Electrospray ionization−mass spectrometry (ESI-MS) was uninformative. However, the former (L = H₂) would form under the conditions of hydrogen production in a sealed tube, and the absence of a Rh−H signal could be due to rapid hydride/dihydrogen exchange.⁸⁵ An alternative explanation is that **8** is a neutral Rh species that does not contain a hydride, formed by deprotonation of the Rh−H group.

These NMR data are similar to those reported for the phosphino−borane complexes such as [Rh(κ²-ₚₚ-PPh₂(CH₂)₃PPh₂)(H)(PPh₂BH₃)(H₃B·PPh₂H)][BArF₄]

Scheme 15. Tentative Structure for Intermediate Complex 8
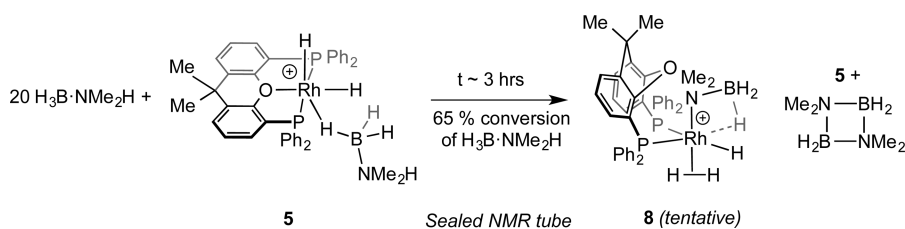
(Scheme 3b),[45,47] in particular, the large $^1H-^{31}P$ *trans* coupling and chemical shift for the proposed β-agostic BH unit (δ -6.9, $J(PH)$ 77 Hz) and the chemical shifts in the $^{31}P\{^1H\}$ NMR spectrum for the chelating phosphine (δ 10.5 $J(RhP)$ 102 Hz; 27.2, δ $J(RhP)$ 131 Hz). The assigned β-agostic BH group also comes at a chemical shift similar to that observed for other agostic Rh⋯HBN interactions, for example, in the dimer $[Rh_2(P^iPr_3)_2(H)_2(\sigma, \mu-H_2BNMe_3)(\mu-H_3B\cdot NMe_3)][BAr^F_4]_2$ (δ -9.46).[62] A possible mode of formation of **8** from **5** could involve NH proton transfer to the hydride (protonlysis). A similar process has been suggested by computation for NH activation in $H_3B\cdot NH_3$ by (Cy-PSiP)RuN(SiMe_3) (CyPSiP = $\kappa^3-(Cy_2PC_6H_4)_2SiMe$).[86] Similar ^1H and $^{31}P\{^1H\}$ NMR spectra to **8** are also observed at early stages of reaction when $H_3B\cdot NMeH_2$ is used with **1** in the dehydropolymerization, with **7** also observed. However, these species very quickly disappear to be replaced by multiple very broad signals between δ -8 and -10 and broad signals in the $^{31}P\{^1H\}$ NMR spectrum, suggestive of multiple species being present during catalysis, possibly species with growing polymeric units. We have not been successful in our attempts to isolate any of these intermediates, as in the absence of excess amine−borane, only the dihydride precursors (i.e., **5** and **7**) are observed alongside the boron-containing products of dehydrogenation. This might suggest the N−H activation is a cooperative process, possibly involving N−H⋯H−B dihydrogen bonds.[87]

Although we cannot fully discount an alternative formulation for **8** as base-stabilized boryl (e.g., $Rh(H)BH_2NMe_2H$),[62] the temporal evolution of **8** is inconsistent with this, as B−H exchange is rapid (Section 2.1) compared to the induction period. Moreover, the induction period changes on NH/ND exchange, while not with BH/BD exchange, further suggesting N−H activation is important in the formation of the catalytically competent intermediate. Likewise, the NMR data do not allow us to discount a dimeric structure for **8**. Such a motif has not been reported for [Rh(Xantphos)] complexes, and only a handful of examples with Ir, Pd, and Au are known for this ligand.[88−91] The Ir complexes, e.g., $[Ir(\kappa^3-_{POP}-Xantphos)(H)(\mu-H)]_2[BAr^F_4]$,[88] contain bridging hydrides that show large *trans* coupling to two ^{31}P environments, different to that observed for **8**.

We sought additional evidence for the formation of an Rh−amido−hydride arising from N−H activation, by use of $Et_3B\cdot NMe_2H$.[92] This substrate has B−H functionality blocked and thus acts as a potential probe for N−H activation only, and such an approach has recently been used in Ru(HPNP)-(H)_2(PMe_3) systems to generate amido−borane species in low relative concentration.[23] In our hands, the reaction ultimately leads to the product of B−N bond cleavage, $[Rh(\kappa^3-_{P,O,P}-Xantphos)(H)_2(NMe_2H)][BAr^F_4]$, **9** (Scheme 16), a complex that has been characterized by NMR spectroscopy and also independently synthesized by addition of NMe_2H to **2** (Supporting Information). No intermediate species were observed, and the fate of the borane has not been investigated.

Scheme 16. Reactivity of $Et_3B\cdot NMe_2H$ with 2
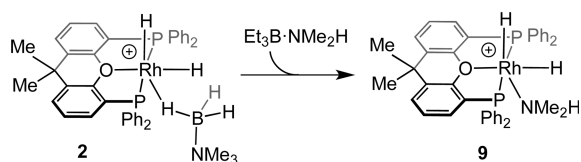
The tentative, suggested structure of **8**, with an amido−borane motif, has precedent with mechanistic studies on other amine−borane dehydrogenation catalyst systems: for example, group 2 catalysts, which invoke very similar intermediates for $H_3B\cdot NMe_2H$ (and related) dehydrogenation;[81,93,94] Fe-based systems in which such motifs have been suggested to be key intermediates for the propagation of a polymer chain in $H_3B\cdot NH_3$ dehydropolymerization;[22] and Cp_2Ti^{28} or Rh-$(PCy_3)_2(H)_2Cl^{67}$ catalysts for dehydrocoupling of $H_3B\cdot NMe_2H$. Moreover, closely related phosphido−borane species have been isolated and shown to be productive intermediates in phosphine borane dehydrocoupling.[45]

2.2.9. Alternative Aminoboryl Complex as a Possible Resting State? An alternate identity of **CAT−AB** we have considered is a complex in which B−H activation has occurred through reaction with the amino−borane product, to give a hydridoboryl complex.[95] To explore this possibility, addition of a large excess (20 equiv) of the monomeric and stable $H_2B=N^iPr_2$[96] to **2** resulted in the immediate formation of a new product that was tentatively characterized as $[Rh(\kappa^3-_{POP}-Xantphos)(H)(BH=N^iPr_2)(H_3B\cdot NMe_3)][BAr^F_4]$, **10a**, alongside **2** in a ratio of 5:1. NMR data are fully consistent with this formulation; in particular, only one environment is observed, namely, δ 39.6 ($J(RhP)$ = 126 Hz) in the $^{31}P\{^1H\}$ NMR spectrum. In the ^1H NMR spectrum, a single hydride peak is observed at δ -14.15 (br multiplet) that sharpens on decoupling ^{31}P to reveal a doublet ($J(RhH)$ = 33 Hz) and a broad signal at δ 0.06. The chemical shift of the hydride is not particularly high field, suggesting that it does not lie *trans* to a vacant site,[97] e.g., the 14-electron amino−boryl [Rh-$(IMes)_2(H)(B(H)NMe_2)][BAr^F_4]$ δ -23.6,[98] rather being more like a "Y-shaped"[99] 16-electron structure. For example, the hydrido ligand in the Y-shaped hydrido−boryl RhHCl-$(Bcat)(P^iPr_3)_2$ (cat =1,2-O_2C_6H_4) is observed at δ -17.08.[100] In the ^{11}B NMR spectrum, a broad signal at δ 49 is observed, consistent with an amino−boryl unit.[95,98] Attempts to isolate this material as a solid resulted in decomposition. However, addition of MeCN to the mixture containing **10a** results in the formation of the corresponding MeCN adduct: $[Rh(\kappa^3-_{POP}-Xantphos)(H)(BH=N^iPr_2)(NCMe)][BAr^F_4]$, **10c**, which has sufficient stability to be crystallographically characterized (Figure 2), alongside **3** in a 7:1 ratio. The ^1H NMR data for **10c** are fully consistent with the solid-state structure, notably a hydride signal at δ -14.22 (doublet of triplets) and a signal at δ 6.75 that is assigned to the BH group that sharpens on decoupling ^{11}B. The boryl ligand is observed as a broad signal in the ^{11}B NMR spectrum at δ 49. The Rh−B distance in **10c** (2.034(3) Å) is similar to that measured in $[Rh(IMes)_2(H)-(B(H)NMe_2)][BAr^F_4]$ as determined by X-ray diffraction, 1.960(9) Å.[98]

Addition of 15 equiv of $[H_2BNMe_2]_2$, **II**, (a source of $H_2B=NMe_2$[66]) to **2** resulted in a similar complex to **10a** being formed, $[Rh(\kappa^3-_{POP}-Xantphos)(H)(BH=NMe_2)(H_3B\cdot NMe_3)][BAr^F_4]$, **10b** (Scheme 17 and Supporting Information), but now over a longer time scale of 16 h, presumably as the rate-limiting step is the dissociation of **II**.[66] This reaction did not go to completion, and a mixture of **2/10b** in a 1:1 ratio is formed. We could not form **10b** (or **10a**) free of **2**, suggesting an equilibrium is established between the two. In addition, the reaction also shows some other, minor products. Placing this 50:50 mixture of **2/10b** under the conditions of catalysis ($H_3B\cdot NMe_2H$, 0.2 mol % total [Rh], open system, 1,2-$F_2C_6H_2$) resulted in both a similar induction period being
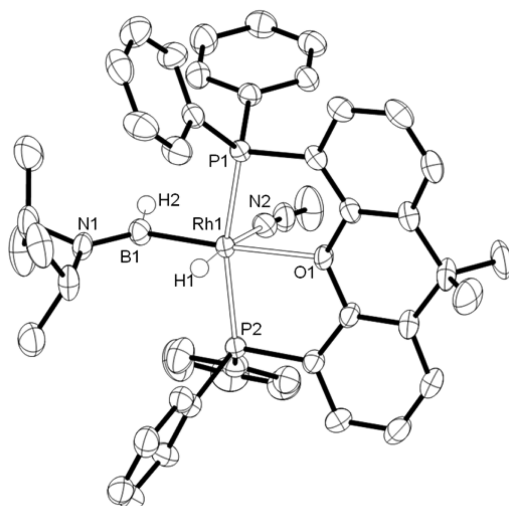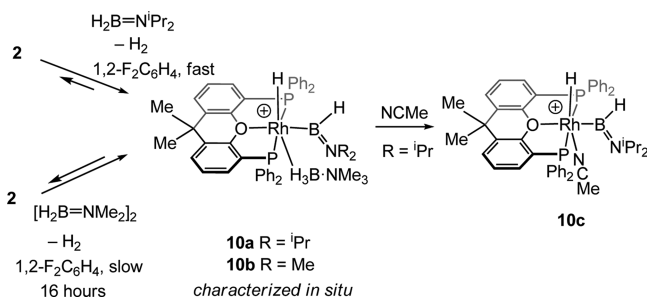
Figure 2. Solid-state structure of the cation in **10c** showing displacement ellipsoids at the 50% probability level. Selected bond lengths (Å) and angles (deg): Rh1−B1, 2.034(3); Rh1−P1, 2.2681(7); Rh1−P2, 2.2684(7); Rh1−O1, 2.2842(17); Rh1−N2, 2.135(2); B1−N1, 1.378(4); B1−Rh1−O, 175.53(11); B1−Rh1−P1, 96.53(10); B1−Rh1−P2, 100.17(10); N1−B1−Rh1, 133.9(2).

Scheme 17. Synthesis of the Hydridoboryl Complexes

observed (400 s) and a similar overall time to completion compared with starting from **1** or **2**, suggesting that **10b** is not the active catalyst species. That the NMR data for **10a** and **10b** are different from that observed for the resting state in solution (i.e., **8**), coupled with observation of this induction period, argues *against* a hydridoboryl structure for **CAT** or **CAT−AB**. The isolation and observation of B−H activated products **10c** and **10b**, respectively, importantly demonstrate that amino−borane fragments can interact with the {Rh(Xantphos)}+ fragment, presumably via an (unobserved) σ-amino−borane complex. Such interactions are suggested to be important in the mechanism of dehydrocoupling as discussed next.

3. DISCUSSION

Within the parameters explored by our experiments, $H_3B \cdot NMe_2H$ and $H_3B \cdot NMeH_2$ show very similar kinetic behavior in their consumption during catalysis, although the final products differ. This suggests that there is a common mechanistic framework that links the two, although certain details will be different, for example, in the final products of the B−N bond forming event. Any mechanistic scenario suggested is required to satisfy a number of criteria that flow from our observations on these two systems: (i) there is a slow induction period, which is proposed to involve N−H activation; (ii) catalysis appears to occur in the Rh(III) oxidation state, rather than a Rh(I)/Rh(III) cycle; (iii) polymer kinetics support a

predominately chain-growth process, there is a single-site model for polymer propagation, and the catalyst is not living; (iv) chain transfer/termination is modified by H_2 and THF, the former resulting in shorter polymer chains, the latter in longer chains; (v) saturation kinetics operate during the productive phase of catalysis, that is, pseudo-zero-order in substrate during the early phase of productive catalysis; (vi) in a sealed system (i.e., under H_2) turnover is slower and follows a first-order decay (as measured for $H_3B \cdot NMe_2H$); and this inhibition by H_2 is reversible, as opening the closed system (i.e., release of H_2) results in an increase in relative rate; (vii) at low substrate concentration, borazine forms, and exogenous cyclohexene is hydroborated, indicating free amino−borane; (viii) at high substrate concentration, no borazine forms, and cyclohexene is not hydroborated; (ix) catalytic turnover proceeds via a resting state that is *suggested* to be an amido−borane; (x) immediately at the end of catalysis, activity is retained in both closed and open systems.

We propose the mechanism shown in Scheme 18 as one that best fits the available data. Addition of amine−borane to **1** results in rapid dehydrogenation and hydrogen transfer to the metal, presumably via a transient sigma complex **A**, to give a Rh(III) dihydride (e.g., **5**). This can also be accessed by direct addition of amine−borane to the preformed Rh(III) complex **2**. Subsequent slow N−H activation results in the formation of the proposed amido−borane **CAT** that can rapidly but reversibly combine with additional amine−borane to form **CAT−AB**. **CAT−AB** then undergoes further NH/BH transfers involving turnover limiting N−H activation. For $H_3B \cdot NMe_2H$, this results in the production of amino−borane $H_2B=NMe_2$ that subsequently dimerizes to give **II**. For $H_3B \cdot NMeH_2$, there is an accompanying B−N bond-forming event that results in a propagating polymer chain on the metal center. We cannot completely discount a similar process occurring for $H_3B \cdot NMe_2H$, as shown for Cp_2Ti,[28] $[Rh(PR_3)_2]^+$,[27,51,58] and group 2 catalysts,[81] which give $H_3B \cdot NMe_2BH_2 \cdot NMe_2H$. However, if this is occurring, B−N bond cleavage must be kinetically competitive as, unlike these other systems, we see no significant amounts of $H_3B \cdot NMe_2BH_2 \cdot NMe_2H$, either free or metal bound. There are systems in which this diborazane has been suggested not to be involved as an intermediate,[18,21] which also dehydropolymerize $H_3B \cdot NMeH_2$.

Although we can only speculate as to the likely intermediates/transition states during these turnover-limiting processes, especially as complex **8** is not fully characterized, a key requirement for $H_3B \cdot NMeH_2$ dehydropolymerization is that any suggested pathway results in overall insertion of an amino−borane unit, as this provides a template for a growing polymer chain at a metal single site, that is, a chain-growth mechanism. In addition, at high $H_3B \cdot NMeH_2$ concentration, free amino−borane is not produced in a kinetically significant amount based upon cyclohexene trapping experiments. We suggest one possible mechanism for the B−N bond-forming event as shown in Scheme 19, in which relatively slower dehydrogenation of $H_3B \cdot NMeH_2$ (with N−H activation being rate limiting) affords a weakly bound "real monomer" amino−borane[101] that then undergoes rapid B−N bond formation. A key component of this mechanism is that the Rh−amido−borane motif is retained throughout and that the B−N bond forming process results in formal insertion of the amino−borane into the Rh−N bond. We are unable to comment on the precise coordination motif of the Xantphos ligand during

Scheme 18. Suggested Mechanistic Cycle and Intermediates for the Dehydrocoupling of H₃B·NMe₂H and the Dehydropolymerization of H₃B·NMeH₂[a]
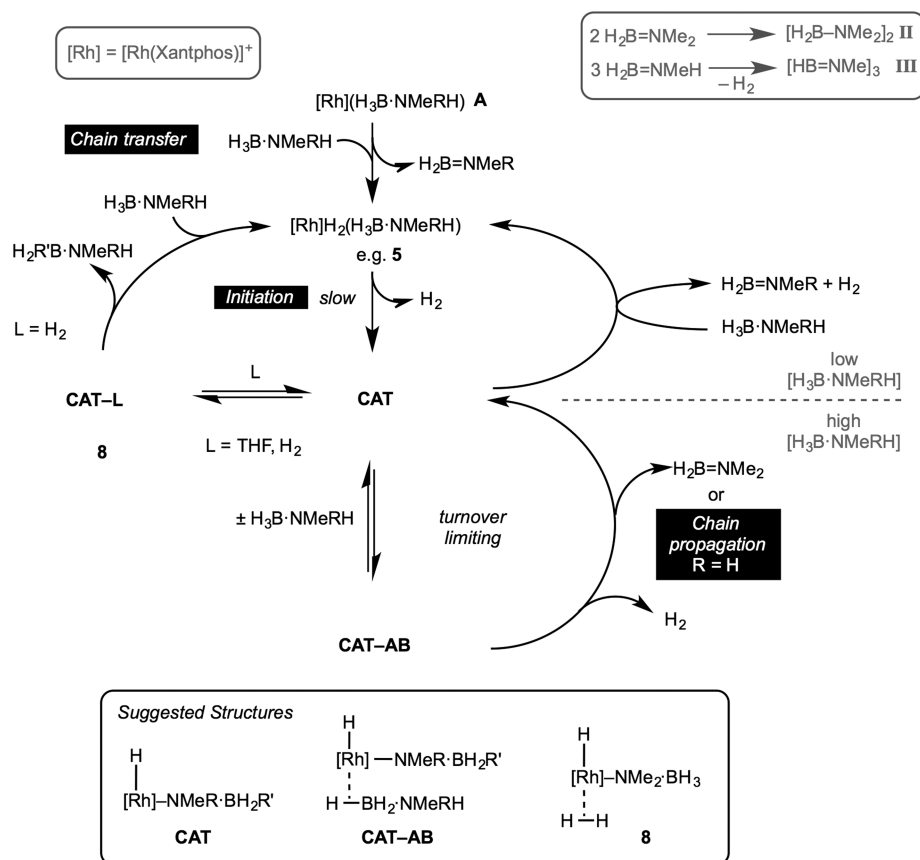
[a]For H₃B·NMeH₂, R′ = H or growing polymer chain, R = H. For H₃B·NMe₂H, R = Me, R′ = H.

Scheme 19. Postulated Pathway, Based upon the Suggested Intermediates, for the B–N Coupling Event in H₃B·NMeH₂ Dehydropolymerization[a]
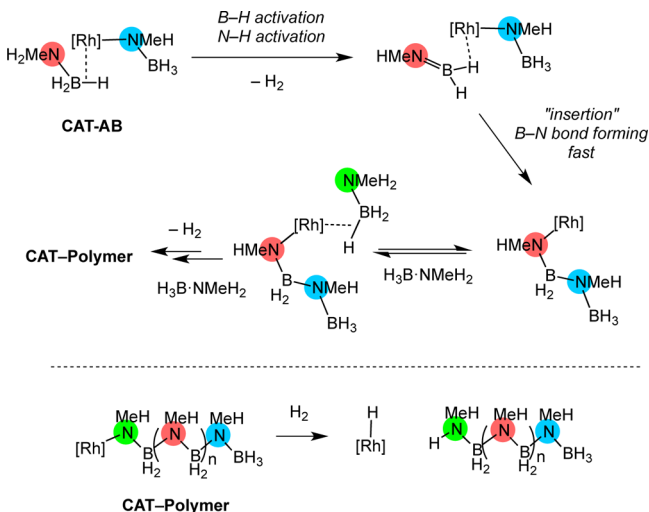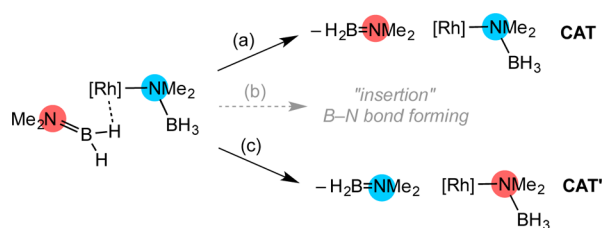

[a][Rh] = [Rh(Xantphos)(H)]⁺.

these steps, as κ^2-P,P and κ^3-P,O,P coordination modes are both accessible.[53,54]

Dihydrogen acts as a chain-transfer agent. At lower H₃B·NMeH₂ concentration or high H₂ concentration under sealed tube conditions, binding of H₂ could well become competitive

with amine–borane coordination in **CAT–polymer**. Chain termination by heterolytic cleavage[102] of the coordinated H₂ could return a Rh(III)H₂ fragment (i.e., **5**) and the free polymer. We suggest that THF also acts to modify the catalyst by binding competitively with both H₂ and amine–borane (i.e., **CAT–L**, Scheme 18). This slows down productive catalysis but also attenuates chain transfer, so that longer polymer chains result. Under stoichiometric conditions of low concentration of H₃B·NMeH₂, borazine **III** is formed. This could either occur from **5** by successive slow BH/NH transfer steps or from **CAT** that under such conditions would find no stabilization from additional amine–borane and could undergo B–H β-hydrogen transfer to form H₂B=NMeH (that then trimerizes/loses H₂) and a RhH₂ species. Consistent with the formation of amino–borane at low H₃B·NMeH₂ concentration, cyclohexene is hydroborated under these conditions.

This general mechanistic scheme can also be used to speculate upon the dehydrogenation pathway of the secondary amine–borane H₃B·NMe₂H. Formation of **CAT–AB** and BH/NH transfer leads to an amino–borane intermediate (Scheme 20) but now with H₂B=NMe₂ bound. This can simply either lose the bulkier H₂B=NMe₂ fragment that then dimerizes to form **II** (pathway a) or undergo an H-transfer process[103] from BH₃ to BH₂ to generate an alternate amido–borane and free H₂B=NMe₂ (pathway c). With the current data in hand, we cannot discriminate between these two processes. We suggest that B–N coupling in the secondary amine–borane is disfavored due to steric grounds (pathway b), as we have

Scheme 20. Postulated Pathways for the Dehydrocoupling of $H_3B \cdot NMe_2H$[a]

[a][Rh] = [Rh(Xantphos)]$^+$.

recently explored in the formation (or lack of) oligomeric amino−boranes on $[Ir(PCy_3)(H)_2]^+$ fragments with $H_3B \cdot NH_3$ (oligomers), $H_3B \cdot NMeH_2$ (linear dimer), and $H_3B \cdot NMe_2H$ (amino−borane), in which sterics play an important role.[104]

4. CONCLUSIONS

A detailed mechanistic study on the dehydrocoupling of $H_3B \cdot NMe_2H$ and dehydropolymerization of $H_3B \cdot NMeH_2$ using the $[Rh(Xantphos)]^+$ fragment suggests that similar mechanisms operate for both, which only differ in that B−N bond formation (and the resulting propagation of a polymer chain) is favored for $H_3B \cdot NMeH_2$ but not $H_3B \cdot NMe_2H$. The key feature of this suggested mechanism is the generation of an active catalyst, proposed to be an amido−borane, that then reversibly binds additional amine−borane so that saturation kinetics operate during catalysis. B−N bond formation (with $H_3B \cdot NMeH_2$) or elimination of amino−borane (with $H_3B \cdot NMe_2H$) follows. Importantly, for the dehydropolymerization of $H_3B \cdot NMeH_2$, we also demonstrate that polymer formation follows chain-growth processes from the metal and that control of polymer molecular weight can also be achieved by using H_2 or THF solvent. Hydrogen is suggested to act as a chain-transfer agent, leading to low-molecular-weight polymer; while THF acts to attenuate chain transfer, and accordingly, longer polymer chains are formed. Although the molecular weights of polymeric material obtained are still rather modest compared to the previously reported $Ir(^tBuPOCOP^tBu)(H)_2$ system, the insight available from using the valence isoelectronic $[Rh(Xantphos)-(H)_2]^+$ fragment leads to a mechanistic framework that explains the experimental observations and polymer growth kinetics. The suggested mechanism for dehydropolymerization is one in which the putative amido−borane species dehydrogenates an additional $H_3B \cdot NMeH_2$ to form the "real monomer" $H_2B{=}NMeH$ that then undergoes insertion into the Rh−amido bond to propagate the growing polymer chain on the metal. This is directly analogous to the chain-growth mechanism for single-site olefin polymerization.[1] A future challenge is thus to use this insight to develop catalysts capable of living polymerization and/or control of polymer tacticity as so elegantly demonstrated with polyolefin chemistry; it will be interesting to see whether the mechanistic themes discussed here are applicable in a more general sense to other catalyst systems.

ASSOCIATED CONTENT

Ⓢ Supporting Information

Experimental and characterization details, including NMR data, X-ray crystallographic data, polymer characterization data and kinetic plots. This material is available free of charge via the Internet at http://pubs.acs.org. Crystallographic data have been deposited with the Cambridge Crystallographic Data Center (CCDC) and can be obtained via www.ccdc.cam.ac.uk/data_request/cif.

AUTHOR INFORMATION

Corresponding Authors

ian.manners@bristol.ac.uk
guy.lloyd-jones@ed.ac.uk
andrew.weller@chem.ox.ac.uk

Notes

The authors declare no competing financial interest.

REFERENCES

(1) Hartwig, J. F. *Organotransition Metal Chemistry: From Bonding to Catalysis*; University Science Books: Sausalito, Calif., 2010.
(2) Leitao, E. M.; Jurca, T.; Manners, I. *Nat. Chem.* **2013**, *5*, 817−829.
(3) Waterman, R. *Chem. Soc. Rev.* **2013**, *42*, 5629−5641.
(4) Clark, T. J.; Lee, K.; Manners, I. *Chem.—Eur. J.* **2006**, *12*, 8634−8648.
(5) Hansmann, M. M.; Melen, R. L.; Wright, D. S. *Chem. Sci.* **2011**, *2*, 1554−1559.
(6) Pons, V.; Baker, R. T. *Angew. Chem., Int. Ed.* **2008**, *47*, 9600−9602.
(7) Liu, Z.; Song, L.; Zhao, S.; Huang, J.; Ma, L.; Zhang, J.; Lou, J.; Ajayan, P. M. *Nano Lett.* **2011**, *11*, 2032−2037.
(8) Komm, R.; Geanangel, R. A.; Liepins, R. *Inorg. Chem.* **1983**, *22*, 1684−1686.
(9) Schaeffer, G. W.; Adams, M. D.; Koenig, F. J.; Koenig, S. J. *J. Am. Chem. Soc.* **1956**, *78*, 725−728.
(10) McGee, H. A.; Kwon, C. T. *Inorg. Chem.* **1970**, *9*, 2458−2461.
(11) Kim, D.-P.; Moon, K.-T.; Kho, J.-G.; Economy, J.; Gervais, C.; Babonneau, F. *Polym. Adv. Technol.* **1999**, *10*, 702−712.
(12) Göttker-Schnetmann, I.; White, P.; Brookhart, M. *J. Am. Chem. Soc.* **2004**, *126*, 1804−1811.
(13) Denney, M. C.; Pons, V.; Hebden, T. J.; Heinekey, D. M.; Goldberg, K. I. *J. Am. Chem. Soc.* **2006**, *128*, 12048−12049.
(14) St. John, A.; Goldberg, K. I.; Heinekey, D. M. *Top. Organomet. Chem.* **2013**, *40*, 271−287.
(15) Staubitz, A.; Sloan, M. E.; Robertson, A. P. M.; Friedrich, A.; Schneider, S.; Gates, P. J.; Schmedt auf der Günne, J.; Manners, I. *J. Am. Chem. Soc.* **2010**, *132*, 13332−13345.
(16) Dietrich, B. L.; Goldberg, K. I.; Heinekey, D. M.; Autrey, T.; Linehan, J. C. *Inorg. Chem.* **2008**, *47*, 8583−8585.
(17) Staubitz, A.; Presa Soto, A.; Manners, I. *Angew. Chem., Int. Ed.* **2008**, *47*, 6212−6215.
(18) Vance, J. R.; Robertson, A. P. M.; Lee, K.; Manners, I. *Chem.—Eur. J.* **2011**, *17*, 4099−4103.
(19) Kakizawa, T.; Kawano, Y.; Naganeyama, K.; Shimoi, M. *Chem. Lett.* **2011**, *40*, 171−173.
(20) Kawano, Y.; Uruichi, M.; Shimoi, M.; Taki, S.; Kawaguchi, T.; Kakizawa, T.; Ogino, H. *J. Am. Chem. Soc.* **2009**, *131*, 14946−14957.
(21) Dallanegra, R.; Robertson, A. P. M.; Chaplin, A. B.; Manners, I.; Weller, A. S. *Chem. Commun.* **2011**, *47*, 3763−3765.
(22) Baker, R. T.; Gordon, J. C.; Hamilton, C. W.; Henson, N. J.; Lin, P.-H.; Maguire, S.; Murugesu, M.; Scott, B. L.; Smythe, N. C. *J. Am. Chem. Soc.* **2012**, *134*, 5598−5609.
(23) Marziale, A. N.; Friedrich, A.; Klopsch, I.; Drees, M.; Celinski, V. R.; Schmedt auf der Günne, J.; Schneider, S. *J. Am. Chem. Soc.* **2013**, *135*, 13342−13355.
(24) Wright, W. R. H.; Berkeley, E. R.; Alden, L. R.; Baker, R. T.; Sneddon, L. G. *Chem. Commun.* **2011**, *47*, 3177−3179.
(25) Ewing, W. C.; Carroll, P. J.; Sneddon, L. G. *Inorg. Chem.* **2013**, *52*, 10690−10697.

(26) Himmelberger, D. W.; Yoon, C. W.; Bluhm, M. E.; Carroll, P. J.; Sneddon, L. G. *J. Am. Chem. Soc.* **2009**, *131*, 14101−14110.

(27) Sewell, L. J.; Lloyd-Jones, G. C.; Weller, A. S. *J. Am. Chem. Soc.* **2012**, *134*, 3598−3610.

(28) Sloan, M. E.; Staubitz, A.; Clark, T. J.; Russell, C. A.; Lloyd Jones, G. C.; Manners, I. *J. Am. Chem. Soc.* **2010**, *132*, 3831−3841.

(29) Friedrich, A.; Drees, M.; Schneider, S. *Chem.—Eur. J.* **2009**, *15*, 10339−10342.

(30) Alcaraz, G.; Sabo-Etienne, S. *Angew. Chem., Int. Ed.* **2010**, *49*, 7170−7179.

(31) Staubitz, A.; Robertson, A. P. M.; Sloan, M. E.; Manners, I. *Chem. Rev.* **2010**, *110*, 4023−4078.

(32) Roselló-Merino, M.; López-Serrano, J.; Conejero, S. *J. Am. Chem. Soc.* **2013**, *135*, 10910−10913.

(33) Vance, J. R.; Schäfer, A.; Robertson, A. P. M.; Lee, K.; Turner, J.; Whittell, G. R.; Manners, I. *J. Am. Chem. Soc.* **2014**, *136*, 3048−3064.

(34) Robertson, A. P. M.; Leitao, E. M.; Jurca, T.; Haddow, M. F.; Helten, H.; Lloyd-Jones, G. C.; Manners, I. *J. Am. Chem. Soc.* **2013**, *135*, 12670−12683.

(35) Induction periods in amine−borane dehydrocoupling can be indicative of the formation of active nanoparticle catalysts: (a) Jaska, C. A.; Manners, I. *J. Am. Chem. Soc.* **2004**, *126*, 9776−9785. (b) Sonnenberg, J. F.; Morris, R. H. *ACS Catal.* **2013**, *3*, 1092−1102.

(36) Lu, Z.; Conley, B. L.; Williams, T. J. *Organometallics* **2012**, *31*, 6705−6714.

(37) Pons, V.; Baker, R. T.; Szymczak, N. K.; Heldebrant, D. J.; Linehan, J. C.; Matus, M. H.; Grant, D. J.; Dixon, D. A. *Chem. Commun.* **2008**, 6597−6599.

(38) Free H$_2$B=NMeH or H$_2$B=NH$_2$ have only been observed at low temperature: (a) Carpenter, J. D.; Ault, B. S. *J. Phys. Chem.* **1991**, *95*, 3507−3511. (b) Kwon, C. T.; McGee, H. A. *Inorg. Chem.* **1970**, *9*, 2458−2461. Such compounds can be trapped by dehydrogenation of the corresponding amine−borane and coordination to a metal center, (c) Alcaraz, G.; Vendier, L.; Clot, E.; Sabo-Etienne, S. *Angew. Chem., Int. Ed.* **2010**, *49*, 918−920. or isolated by formation of a donor−acceptor complex. (d) Malcolm, A. C.; Sabourin, K. J.; McDonald, R.; Ferguson, M. J.; Rivard, E. *Inorg. Chem.* **2012**, *51*, 12905−12916.

(39) (a) Johnson, H. C.; Weller, A. S. *J. Organomet. Chem.* **2012**, *721−722*, 17−22. (b) Leitao, E. M.; Stubbs, N. E.; Robertson, A. P. M.; Helten, H.; Cox, R. J.; Lloyd-Jones, G. C.; Manners, I. *J. Am. Chem. Soc.* **2012**, *134*, 16805−16816.

(40) Malakar, T.; Roy, L.; Paul, A. *Chem.—Eur. J.* **2013**, *19*, 5812−5817.

(41) Hebden, T. J.; Denney, M. C.; Pons, V.; Piccoli, P. M. B.; Koetzle, T. F.; Schultz, A. J.; Kaminsky, W.; Goldberg, K. I.; Heinekey, D. M. *J. Am. Chem. Soc.* **2008**, *130*, 10812−10820.

(42) Johnson, H. C.; Robertson, A. P. M.; Chaplin, A. B.; Sewell, L. J.; Thompson, A. L.; Haddow, M. F.; Manners, I.; Weller, A. S. *J. Am. Chem. Soc.* **2011**, *133*, 11076−11079.

(43) Shimoi, M.; Nagai, S.; Ichikawa, M.; Kawano, Y.; Katoh, K.; Uruichi, M.; Ogino, H. *J. Am. Chem. Soc.* **1999**, *121*, 11704−11712.

(44) Dorn, H.; Singh, R. A.; Massey, J. A.; Nelson, J. M.; Jaska, C. A.; Lough, A. J.; Manners, I. *J. Am. Chem. Soc.* **2000**, *122*, 6669−6678.

(45) Huertos, M. A.; Weller, A. S. *Chem. Sci.* **2013**, *4*, 1881−1888.

(46) Huertos, M. A.; Weller, A. S. *Chem. Commun.* **2012**, *48*, 7185−7187.

(47) Hooper, T. N.; Huertos, M. A.; Jurca, T.; Pike, S. D.; Weller, A. S.; Manners, I. *Inorg. Chem.* **2014**, *53*, 3716−3729.

(48) Kranenburg, M.; van der Burgt, Y. E. M.; Kamer, P. C. J.; van Leeuwen, P. W. N. M.; Goubitz, K.; Fraanje, J. *Organometallics* **1995**, *14*, 3081−3089.

(49) Julian, L. D.; Hartwig, J. F. *J. Am. Chem. Soc.* **2010**, *132*, 13813−13822.

(50) Johnson, H. C.; McMullin, C. L.; Pike, S. D.; Macgregor, S. A.; Weller, A. S. *Angew. Chem., Int. Ed.* **2013**, *52*, 9776−9780.

(51) Douglas, T. M.; Chaplin, A. B.; Weller, A. S.; Yang, X. Z.; Hall, M. B. *J. Am. Chem. Soc.* **2009**, *131*, 15440−15456.

(52) Dallanegra, R.; Chaplin, A. B.; Weller, A. S. *Angew. Chem., Int. Ed.* **2009**, *48*, 6875−6878.

(53) Dallanegra, R.; Chaplin, A. B.; Weller, A. S. *Organometallics* **2012**, *31*, 2720−2728.

(54) Williams, G. L.; Parks, C. M.; Smith, C. R.; Adams, H.; Haynes, A.; Meijer, A. J. H. M.; Sunley, G. J.; Gaemers, S. *Organometallics* **2011**, *30*, 6166−6179.

(55) Pawley, R. J.; Moxham, G. L.; Dallanegra, R.; Chaplin, A. B.; Brayshaw, S. K.; Weller, A. S.; Willis, M. C. *Organometallics* **2010**, *29*, 1717−1728.

(56) Haibach, M. C.; Wang, D. Y.; Emge, T. J.; Krogh-Jespersen, K.; Goldman, A. S. *Chem. Sci.* **2013**, *4*, 3683−3692.

(57) Esteruelas, M. A.; Oliván, M.; Vélez, A. *Inorg. Chem.* **2013**, *52*, 5339−5349.

(58) Chaplin, A. B.; Weller, A. S. *Inorg. Chem.* **2010**, *49*, 1111−1121.

(59) Complex **4** could be obtained as the only organometallic complex by hydrogenation of the NBD precursor in neat THF. Crystallization afforded oil-covered crystals, for which good solution NMR data could be obtained (see the Supporting Information).

(60) Perutz, R. N.; Sabo-Etienne, S. *Angew. Chem., Int. Ed.* **2007**, *46*, 2578−2592.

(61) Algarra, A. G.; Sewell, L. J.; Johnson, H. C.; Macgregor, S. A.; Weller, A. S. *Dalton Trans.* **2014**, DOI: 10.1039/C3DT52771A.

(62) Chaplin, A. B.; Weller, A. S. *Angew. Chem., Int. Ed.* **2010**, *49*, 581−584.

(63) Rossin, A.; Caporali, M.; Gonsalvi, L.; Guerri, A.; Lledós, A.; Peruzzini, M.; Zanobini, F. *Eur. J. Inorg. Chem.* **2009**, *2009*, 3055−3059.

(64) Yasue, T.; Kawano, Y.; Shimoi, M. *Angew. Chem., Int. Ed.* **2003**, *42*, 1727−1730.

(65) Alcaraz, G.; Sabo-Etienne, S. *Coord. Chem. Rev.* **2008**, *252*, 2395−2409.

(66) Stevens, C. J.; Dallanegra, R.; Chaplin, A. B.; Weller, A. S.; Macgregor, S. A.; Ward, B.; McKay, D.; Alcaraz, G.; Sabo-Etienne, S. *Chem.—Eur. J.* **2011**, *17*, 3011−3020.

(67) Sewell, L. J.; Huertos, M. A.; Dickinson, M. E.; Weller, A. S.; Lloyd-Jones, G. C. *Inorg. Chem.* **2013**, *52*, 4509−4516.

(68) Jaska, C. A.; Temple, K.; Lough, A. J.; Manners, I. *J. Am. Chem. Soc.* **2003**, *125*, 9424−9434.

(69) Narula, C. K.; Janik, J. F.; Duesler, E. N.; Paine, R. T.; Schaeffer, R. *Inorg. Chem.* **1986**, *25*, 3346−3349.

(70) Noth, H.; Vahrenkamp, H. *Chem. Ber./Recl.* **1966**, *99*, 1049−&.

(71) THF is competitive with σ-bound H$_2$ as a ligand in cationic [Rh(PR$_3$)$_2$(H)$_2$(H$_2$)]$^+$ complexes to give the corresponding mono-THF adduct: Ingleson, M. J.; Brayshaw, S. K.; Mahon, M. F.; Ruggiero, G. D.; Weller, A. S. *Inorg. Chem.* **2005**, *44*, 3162−3171.

(72) Within standard error, the degree of polymerization is the same for both. However, we note that, due to the low refractive index difference between poly(methylaminoborane) and the eluent, these errors probably occupy the smaller end of the range (see the Supporting Information).

(73) Alt, H. G.; Köppl, A. *Chem. Rev.* **2000**, *100*, 1205−1222.

(74) It is noteworthy that, in the 0.288 M concentration regime, the catalyst loading is only 0.05 mol %, leading to a ToN of 2000 and a ToF of ∼ 1300 h^{-1}.

(75) Jordan, R. B. *Reaction Mechanisms of Inorganic and Organometallic Systems*; Oxford University Press: New York, 2007.

(76) Due to limitations in our sampling procedure that are a consequence of interrogation by ^{11}B NMR spectroscopy of an open system, we do not have the density of data in this region to be more precise in the changes in the induction period on H/D exchange.

(77) Keaton, R. J.; Blacquiere, J. M.; Baker, R. T. *J. Am. Chem. Soc.* **2007**, *129*, 1844−1845.

(78) Yang, X.; Hall, M. B. *J. Organomet. Chem.* **2009**, *694*, 2831−2838.

(79) Butera, V.; Russo, N.; Sicilia, E. *Chem.—Eur. J.* **2011**, *17*, 14586−14592.

(80) Butera, V.; Russo, N.; Sicilia, E. *ACS Catal.* **2014**, *4*, 1104−1113.

(81) Liptrot, D. J.; Hill, M. S.; Mahon, M. F.; MacDougall, D. J. *Chem.—Eur. J.* **2010**, *16*, 8508−8515.

(82) Spielmann, J.; Piesik, D. F. J.; Harder, S. *Chem.—Eur. J.* **2010**, *16*, 8307−8318.

(83) Forster, T. D.; Tuononen, H. M.; Parvez, M.; Roesler, R. *J. Am. Chem. Soc.* **2009**, *131*, 6689−6691.

(84) Helten, H.; Dutta, B.; Vance, J. R.; Sloan, M. E.; Haddow, M. F.; Sproules, S.; Collison, D.; Whittell, G. R.; Lloyd-Jones, G. C.; Manners, I. *Angew. Chem., Int. Ed.* **2013**, *52*, 437−440.

(85) Douglas, T. M.; Brayshaw, S. K.; Dallanegra, R.; Kociok-Köhn, G.; Macgregor, S. A.; Moxham, G. L.; Weller, A. S.; Wondimagegn, T.; Vadivelu, P. *Chem.—Eur. J.* **2008**, *14*, 1004−1022.

(86) MacInnis, M. C.; McDonald, R.; Ferguson, M. J.; Tobisch, S.; Turculet, L. *J. Am. Chem. Soc.* **2011**, *133*, 13622−13633.

(87) Chen, X.; Zhao, J.-C.; Shore, S. G. *Acc. Chem. Res.* **2013**, *46*, 2666−2675.

(88) Pontiggia, A. J.; Chaplin, A. B.; Weller, A. S. *J. Organomet. Chem.* **2011**, *696*, 2870−2876.

(89) Ito, H.; Saito, T.; Miyahara, T.; Zhong, C.; Sawamura, M. *Organometallics* **2009**, *28*, 4829−4840.

(90) Escalle, A.; Mora, G.; Gagosz, F.; Mezailles, N.; Le, G. X. F.; Jean, Y.; Le, F. P. *Inorg. Chem.* **2009**, *48*, 8415−8422.

(91) van Leeuwen, P. W. N. M.; Zuideveld, M. A.; Swennenhuis, B. H. G.; Freixa, Z.; Kamer, P. C. J.; Goubitz, K.; Fraanje, J.; Lutz, M.; Spek, A. L. *J. Am. Chem. Soc.* **2003**, *125*, 5523−5539.

(92) Landesman, H.; Williams, R. E. *J. Am. Chem. Soc.* **1961**, *83*, 2663−2666.

(93) Bellham, P.; Hill, M. S.; Kociok-Kohn, G.; Liptrot, D. J. *Chem. Commun.* **2013**, *49*, 1960−1962.

(94) Bellham, P.; Hill, M. S.; Kociok-Kohn, G.; Liptrot, D. J. *Dalton Trans.* **2013**, *42*, 737−745.

(95) O'Neill, M.; Addy, D. A.; Riddlestone, I.; Kelly, M.; Phillips, N.; Aldridge, S. *J. Am. Chem. Soc.* **2011**, *133*, 11500−11503.

(96) Euzenat, L.; Horhant, D.; Ribourdouille, Y.; Duriez, C.; Alcaraz, G.; Vaultier, M. *Chem. Commun.* **2003**, 2280−2281.

(97) Hauger, B. E.; Gusev, D.; Caulton, K. G. *J. Am. Chem. Soc.* **1994**, *116*, 208−214.

(98) Tang, C. Y.; Phillips, N.; Bates, J. I.; Thompson, A. L.; Gutmann, M. J.; Aldridge, S. *Chem. Commun.* **2012**, *48*, 8096−8098.

(99) Riehl, J. F.; Jean, Y.; Eisenstein, O.; Pelissier, M. *Organometallics* **1992**, *11*, 729−737.

(100) Westcott, S. A.; Taylor, N. J.; Marder, T. B.; Baker, R. T.; Jones, N. J.; Calabrese, J. C. *J. Chem. Soc., Chem. Commun.* **1991**, 304−305.

(101) Addy, D. A.; Bates, J. I.; Kelly, M. J.; Riddlestone, I. M.; Aldridge, S. *Organometallics* **2013**, *32*, 1583−1586.

(102) Kubas, G. J. *J. Organomet. Chem.* **2014**, *751*, 33−49.

(103) Robertson, A. P. M.; Leitao, E. M.; Manners, I. *J. Am. Chem. Soc.* **2011**, *133*, 19322−19325.

(104) Kumar, A.; Johnson, H. C.; Hooper, T. N.; Weller, A. S.; Algarra, A. G.; Macgregor, S. A. *Chem. Sci.* **2014**, *5*, 2546−2553.